MAP0007: D5.8: Seafloor massive sulphide testing report

18 December 2020

KAVA Reference (Number, Acronym, Full Title):
17034, MAP, Mineral Resource Assessment Platform

Name of the author/Responsible partner:
Steinar Ellefmo and Cyril Juliani / Norwegian University of Science and Technology, NTNU

Version No: 1

This activity has received funding from the European Institute of Innovation and Technology (EIT), a body of the European Union, under the Horizon 2020, the EU Framework Programme for Research and Innovation

Test assessment of the resource potential in the Rainbow area using the MAP Wizard

Ellefmo, S and Juliani, C.
Norwegian University of Science and Technology

Acknowledgments

We would like to acknowledge Kalevi Rasilainen, the GTK-developers and the rest of the MAP-consortium for valuable contributions during the MAP-project and for good and informative discussions during the testing of the MAP Wizard before the assessment workshop. Sven Petersen, Florent Szitkar and Terje Bjerkgård gave valuable contributions during the assessment workshop when they presented various aspects of seafloor massive sulphide genesis and the exploration for such mineralizations. We would like to especially acknowledge Richard Sinding-Larsen, Georgy Cherkashov and Sven Petersen and the rest of the workshop attendees for valuable contributions during the assessment exercise and the discussions. This study was conducted through the MAP project. MAP has received funding from the EIT RAW Materials.

Content

This activity has received funding from the European Institute of Innovation and Technology (EIT), a body of the European Union, under the Horizon 2020, the EU Framework Programme for Research and Innovation

1. Executive summary

This report sums up the assessment of the marine mineral resource potential of seafloor massive sulphide deposits / manifestation yet to be found in a mafic setting inside 9100 km2 large area centred on the Rainbow hydrothermal site.

The work has been part of the Mineral Resource Assessment Platform (MAP) project led by the Finnish geological survey and financially supported by EIT Raw Materials.

The developed tool, the so-called MAP-Wizard is a tool that facilitates the process of assessing the mineral potential inside permissive tracts, or areas outside which there is a negligible probability of finding resources associated to the deposit model under study.

The wizard is applied to quantify the amount of yet-to-find resources. The permissive tracts are defined based on geophysics, backscatter, and structural interpretation of the bathymetric data from the area. The Rainbow area was selected due to the availability of relatively high-resolution data.

Based on expert opinions, one could expect between 4 and 6 hydrothermal manifestations in the area that comply with the defined grade and tonnage model. This grade and tonnage model is based on the relevant onshore analogs (VMS deposits). One could expect that these 4 to 6 deposits on average contain 13.6 Mt @ a median Cu-grade of 2wt%. The permissive area makes up 82% of the total Rainbow area.

The analysis shows that there is an average potential of yet to find resources of 11.4 Mt of ore and 0.2 Mt of Cu associated to a mafic setting. However, the associated uncertainty is significant and future developments should aim at developing more reliable grade tonnage models for these kinds of deposits.

The MAP-Wizard facilitates the assessment process significantly and assist in increasing the transparency of the entire process. However, it is the input that makes the potential assessment reliable or not.

This activity has received funding from the European Institute of Innovation and Technology (EIT), a body of the European Union, under the Horizon 2020, the EU Framework Programme for Research and Innovation

2. Introduction

Marine mineral resources, such as seafloor massive sulfides (SMS), may address future needs in raw materials for nations aiming to sustain industrial and economic development. Past exploration of these seabed resources, which are rich in copper (Cu) and zinc (Zn), and to some degree, gold (Au) and silver (Ag), revealed numbers of depositional sites worldwide in the deep ocean, together with their possible economic significance. Many known, but also unknown, mineral occurrences have uncertain metal tonnage and grade. Addressing these uncertainties is possible with proper evaluation processes, such as the three-part assessment methodology, which requires clear understanding and quantitative analysis of existing geological information. The hereby report present results of the methodology applied to a case study site for evaluating basalt-hosted SMS along the mid-ocean ridge of the Northern Atlantic Ocean.

The methodology applied aims at quantifying speculative and hypothetical resources (USGS, 2009) The resource assessment results presented herein should however due to huge uncertainties in the input data and the implementation of the methodology (e.g., when it comes to the number of deposits) not be taken literally. This work represents more a demonstration of the methodology applied to a deep marine mineral case than a realistic assessment exercise.

2.1. Terminology

Term	Explanation
Mineral deposit	A mineral occurrence of sufficient size and grade that it might, under the most favourable of circumstances, be considered to have economic potential.
Mineral occurrence	A concentration of a mineral (not necessarily, considered in terms of some commodity, such as copper or gold) that is considered valuable by an expert, or that is of scientific interest.
Ore deposit	A mineral deposit that has been tested and is known to be of sufficient size, grade, and accessibility to be producible to yield a profit.
Host-rock	Rocks favourable in forming deposits, as well as source rocks believed to influence the composition of hydrothermal fluids.
Sulphide mineral	Compounds of metals with sulphur, often representing economically important class of minerals. Most major ores of important metals such as copper, lead and silver.

This activity has received funding from the European Institute of Innovation and Technology (EIT), a body of the European Union, under the Horizon 2020, the EU Framework Programme for Research and Innovation

Hydrothermal manifestation	Active hydrothermal venting, indicating the presence of a mineral occurrence.

Seafloor massive sulphides (SMS)

Seafloor massive sulphides represents accumulations of metal sulphide and sulphate minerals, precipitated from hydrothermal vent systems. At seafloor, this precipitation is prominent where a focused outflow of high-temperature hydrothermal fluid (often >300°C for Cu-rich occurrences; Large, 1992) mixes with cold seawater. Related outflow sometimes describes a "black smoke", a metal-rich buoyant plume emitted by sulphide-rich venting chimney structures (Rona, et al., 1986). After successive collapses, resulting fragments pile up to form a mound-shape massive sulphide accumulation below which a network of stringers and veinlets of sulphides, the stockwork, forms in the host rock (Hannington et al., 1998). A prominent amount of sulphide minerals consists of Fe (e.g., pyrite, pyrrhotite and marcasite) but also metals of economic importance such as Cu (e.g., chalcopyrite and isocubanite) and Zn (e.g., sphalerite and wurtzite) (Hannington et al., 1998). Other metals present in lesser quantity, such as Au and Ag, are incorporated as by-products.

Sulphide mounds are subject to a wide spectrum of deposit sizes, morphologies and compositions (Fouquet, 1997; Fouquet et al., 2010; Hannington et al., 2010) depending on subseafloor processes and degrees of preservation. Occurrences developing on the long-term (10s to 100s thousands of years) eventually reach voluminous sizes; e.g., the Trans-Atlantic Geotraverse (TAG) deposit on the Mid-Atlantic Ridge (26°08.2'N, 44°49.6'W) has been estimated to contain nearly 3.9 million tonnes of ores deposited (Hannington et al.,1998) over 5 kyr of intermittent hydrothermal activity and a lifespan of 50 kyr (Lalou et al., 1995). Little is known about the bulk composition, the distribution and geometry of known SMS. However, current knowledge on land-based analogue deposits (volcanogenic massive sulphides or VMS) gives insights on e.g., the geological environments for deposition (e.g., host-rock, age range of mineralization, depositional environment and tectonic setting) and characteristics identifying SMS deposits (e.g., mineralogy, ore textures, alteration patterns, and geochemical or geophysical signatures).

Volcanogenic massive sulphides (VMS)

VMS deposits represent sulphide accumulations where prominent ore minerals, such as Cu-rich chalcopyrite and Zn-rich sphalerite, develop with gangue materials (e.g., pyrite, quartz and barite) (Franklin et al., 2005; Shanks and Thurston, 2010). Such deposits are fossil analogues of presently forming SMS at active hydrothermal vents (Hannington et al., 1998; Franklin et al., 2005; Galley et al., 2007). They are classified as Cyprus-type deposits, i.e. they commonly consist of a conformable massive Cu-Zn ore body developed in ophiolite-related, extrusive basalt sequences (Franklin et al.,

This activity has received funding from the European Institute of Innovation and Technology (EIT), a body of the European Union, under the Horizon 2020, the EU Framework Programme for Research and Innovation

1981; Barrie and Hannington, 1999). Related massive ore, heavily textured by sulphide minerals, grades down into a silicified and pyritic brecciated ore sequence where a sulphide-silicate vein system develop (stockwork). The stockwork includes disseminated pyrites and other sulphide minerals (e.g., chalcopyrite, sphalerite and pyrrhotite) generally observed in relation to an extended chlorite-silica alteration pipe (Craig and Vaughan, 1981; Hannington et al., 1998). Such characteristics can be observed in modern sulphide mounds, but at variable extents since these sulphide mounds are still forming and may differ in bulk mineralogy (e.g., anhydrite is absent in some VMS deposits but present in the TAG sulphide mound; Hannington et al., 1998). With depth, the abundance of sulphide minerals decreases from the massive sulphide horizon to the stockwork base. Related minerals usually consist of, in decreasing order of abundance, a certain proportion of pyrite, chalcopyrite, sphalerite, and pyrrhotite, followed by minor amounts of galena (PbS), tetrahedrite ((Cu,Fe,Zn,Ag)12Sb4S13), tennantite (Cu12As4S13), arsenopyrite (FeAsS), bornite (Cu5FeS4), and magnetite (Fe3O4) (Hannington, 2014).

The size of VMS deposits varies depending on e.g., the volcano-stratigraphic position of the deposit and the tectonic setting of mafic units into which the deposit in question formed; the largest are often located at the contact of separated lava flows or between pillow lavas and the sheeted dike complex (Hannington et al., 1998; Galley and Koski, 1999). Ophiolites in Cyprus and Oman represent typical case studies for examining such evidence (e.g., Adamides, 2010a,b; Gilgen et al., 2014). Respective ore bodies may have been rapidly buried under basaltic lava flows and/or siliceous sedimentary rocks, which prevented them from erosion and/or oxidation below the seafloor.

Ophiolites

Ophiolites are fragments of fossil oceanic lithospheres that first developed at paleo-spreading systems, and then, subsequently obducted onto land after a continued ocean-continent convergence (Dilek, 2003 and references therein). Outcrops of these fragments allow to examine processes that affected related oceanic crust since their genesis. Ophiolites are categorized in terms of tectonic origin and emplacement mechanism (Wakabayashi and Dilek, 2003). A recent paradigm asserted that most of them developed in a supra-subduction zone (SSZ) environment at convergent plate boundaries (Pearce et al., 1984). Precursor definition of an SSZ first derived from geochemical studies conducted by Miyashiro (1973) at the Troodos ophiolite. He described oceanic rocks with geochemical affinities for an island arc magmatism. The model was further attributed to observations that seafloor spreading may form directly above a subducted oceanic lithosphere and present geochemical signatures that differ from mid-ocean ridge (MOR) basalts (MORBs; Pearce et al., 1984). Since the establishment of the concept, SSZ ophiolites are still debated, notably about

This activity has received funding from the European Institute of Innovation and Technology (EIT), a body of the European Union, under the Horizon 2020, the EU Framework Programme for Research and Innovation

e.g., their tectonic setting (among the back-arc to forearc, forearc, oceanic back-arc, and continental back-arc subtypes) and spreading rate at which fossil spreading centers operated (Furnes et al., 2014). Individual ophiolites can differ significantly given their internal structure and stratigraphy, rock assemblages, chemical affinities and mantle sources, in addition to their mode and nature of emplacement (Dilek, 2003; Dilek and Robinson, 2003). Such ophiolites may record a variety of igneous and tectonic origin within orogenic belts representing today suture zones where plate collisions occurred (Nicolas, 1989; Dilek et al., 2000). Well-preserved evidences, such as the Troodos ophiolite on the island of Cyprus (e.g., Cann and Gillis, 2004), are exemplar case studies for understanding processes associated to the formation of Cu-Zn VMS deposits.

This activity has received funding from the European Institute of Innovation and Technology (EIT), a body of the European Union, under the Horizon 2020, the EU Framework Programme for Research and Innovation

3. The MAP Wizard

The MAP-Wizard is an application custom made to facilitate the process of estimating the mineral resource potential or yet-to-find-resources of a certain deposit type inside an area. The application is wrapped around the 3-Part assessment method (Singer and Menzie 2010). The process aims to answer the following questions:

- Where?
  - Where are the permissive tracts (areas) that may contain deposits?
  - A tract is geographically defined so that there is a negligible probability that deposits can be found outside the tract.
- How rich and how big?
  - What are the expected grades and the expected tonnages of the deposits that may be located inside the permissive tracts?
  - To answer this, a grade and tonnage model is normally developed based on known deposits.
- How many?
  - How many deposits satisfying the grade and tonnage model can be found inside the tract (-s).
  - To answer this question one can either run workshops where expert opinions are used or use global density models developed based on previously defined tracts containing a known number of deposits (e.g., Singer and Kouda, 2011).

Figure below (Fig.1) shows the user interface of the MAP Wizard after opening the project. The steps that are facilitated in the wizard are the following:

- Describe the deposit type
- Import the grade and tonnage model relevant to that deposit type
- Delineate the tract
- Define the number of deposits
- Run the Monte Carlo simulation to calculate the yet-to-find resources
- Apply an economic filter to filter out clearly uneconomic deposits
  - This step requires that it is possible to define how the deposit might be mined and associated cost structures.
- Aggregate tract results
  - Relevant only if more than one tract has been defined and analysed

This activity has received funding from the European Institute of Innovation and Technology (EIT), a body of the European Union, under the Horizon 2020, the EU Framework Programme for Research and Innovation

- Report potential estimate results

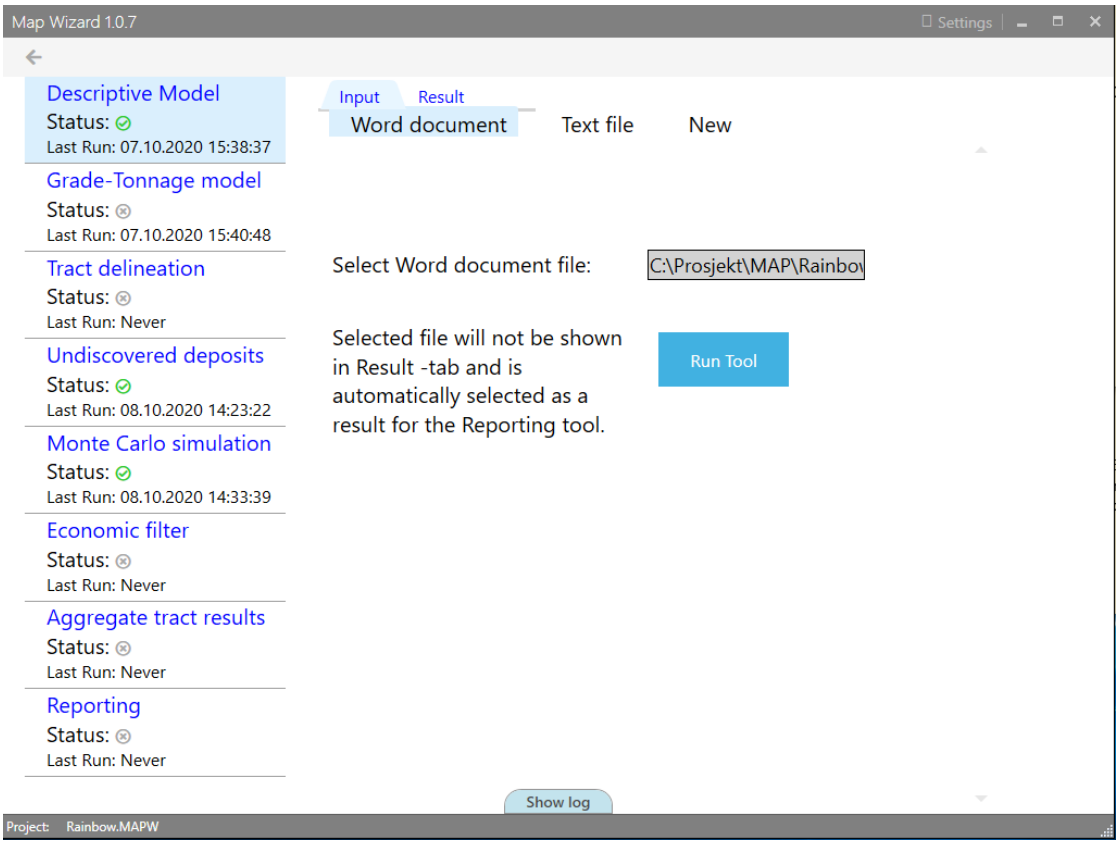

Figure 1. MAP-Wizard user interface

The MAP Wizard is open source and freely available. It can be download from: https://github.com/gtkfi/MapWizard/releases

This activity has received funding from the European Institute of Innovation and Technology (EIT), a body of the European Union, under the Horizon 2020, the EU Framework Programme for Research and Innovation

4. Play analysis

Play-based exploration (see White, 1988, 1993) is a multi-scale exploration technique used to advance the analysis and interpretation of data and build crucial information that mitigate the risk of exploration (e.g., Gautier et al. 1995; Dutton et al. 2003; Attanasi and Freeman 2009). In its application, geological factors, that are critical for the generation of natural resources are documented and mapped in exploration areas. In the context of SMS genesis, factors can include host rocks in which metals accumulate or regional heat sources driving the circulation of metal-rich fluids within the oceanic crust. These factors can be described in the form of a mineral system (Hronsky and Groves 2008; McCuaig and Hronsky 2014; Hagemann et al. 2016) where multi-scale geological processes and corresponding footprints are described and mapped to provide a source-transport-trap analysis that can be used to assess undiscovered mineral deposits (Hagemann et al. 2016). The mapped geological evidence allows the delineation of the most prospective regions (permissive tracts; Singer, 1993), which are then used to map mineral exploration targets at a regional scale (e.g., among the neo-volcanic zones of a MOR; Juliani and Ellefmo, 2018). The play analysis approach has also been used to assess the potential of marine minerals (SMS) inside Norwegian jurisdictions by Ellefmo et al. (2019).

This activity has received funding from the European Institute of Innovation and Technology (EIT), a body of the European Union, under the Horizon 2020, the EU Framework Programme for Research and Innovation

5. Geological setting

5.1. Regional setting, the mid-Atlantic ridge

The Mid-Atlantic Ridge (MAR) represent sites of rising and decompressing of solid mantle where melting and formation of oceanic crust are initiated in response to plate divergence (Wilson, 1989). Melt migrates through large mantellic regions along the ridges and is most often distributed through diking (Fialko and Rubin, 1998). In this process, spreading of newly formed oceanic crust occurs (≤ 55 mm/yr) with frequent magmatism at sites of segmented and localized plume-like magma accretions. Systematic surveying of slow-spreading systems, such as the MAR, revealed prominent morphologies that can be divided in two major domains: (1) the accreting plate boundary zone, i.e. the axial rift valley into which new crustal rocks is formed, and (2) the passive crust, which is moved away off-axis after being generated (Macdonald, 1982). The latter represents high-amplitude abyssal hills formed after subsequent faulting sub-parallel to the ridge axis (Cann et al., 2015). Ridge segments with enhanced magmatism and thickened crust commonly expose a symmetrical faulting pattern on both ridge flanks, while an asymmetric configuration of seafloor spreading is controlled by a spontaneous development of a large-offset normal fault (detachment fault) accommodating a part of the plate separation along one of the ridge flanks (Escartin et al., 2008; Smith et al., 2008, 2014). The volcanic propagation along-axis occurs during periods of high magma supplying to form neo-volcanic zones, which sometimes appear in the form of topographic highs, the axial volcanic ridges (AVRs) (Smith and Cann, 1990; Yeo et al., 2012). Volcanically active zones are now known to host numerous SMS occurrences (Fouquet et al., 2010).

5.2. The Rainbow Area (35 to 37˚N)

The Rainbow Area represents a section of the MAR between 35°40'N and 36°40'N, which consists of slow spreading ridge centres. The overall magmatic input in this area is elevated because of the influence of the nearby Azores hotspot (Detrick et al., 1995; Thibaud et al., 1998; Parson et al., 2000). The ridge is divided into a series of mostly right-stepping ridge segments whose strikes are rotated counter-clockwise to the average strike of the plate boundary: S1, S2, S3 and S4 segments (Fig.2). Non-transform discontinuities (NTDs) comprise the majority of the offsets between ridge segments in this region, including the Rainbow massif which is a discontinuity characterized by nonvolcanic spreading and separating two segment ends (S2 and S3). The massif itself is dome-shaped with a surface composed of ultramafic rocks intermixed with gabbroic intrusions and

This activity has received funding from the European Institute of Innovation and Technology (EIT), a body of the European Union, under the Horizon 2020, the EU Framework Programme for Research and Innovation

variously covered by pelagic and hydrothermal sediments (Andreani et al., 2014). It is considered as an oceanic core complex (OCC) associated to high Bouguer gravity anomaly (Fig.3) (Fouquet et al., 1997; Andreani et al., 2014). The massif hosts a major hydrothermal vent field, the Rainbow hydrothermal field (RHF), composed of several black smokers and other vents (German et al., 2010). The high temperature and high flow rate suggest that the system is driven by a magmatic heat source (Cann and Strens, 1982; Allen and Seyfried, 2004).

Crustal accretion in the Rainbow Area appears dominated by volcanic extension originating from ridge segments in neo-volcanic zones (S1 to S4 in Fig.2), although tectonic extension is locally prominent, next to sedimented basins especially, where seafloor is free of extrusive volcanic morphologies (i.e. detachment zones or OCCs) (Fig.2).

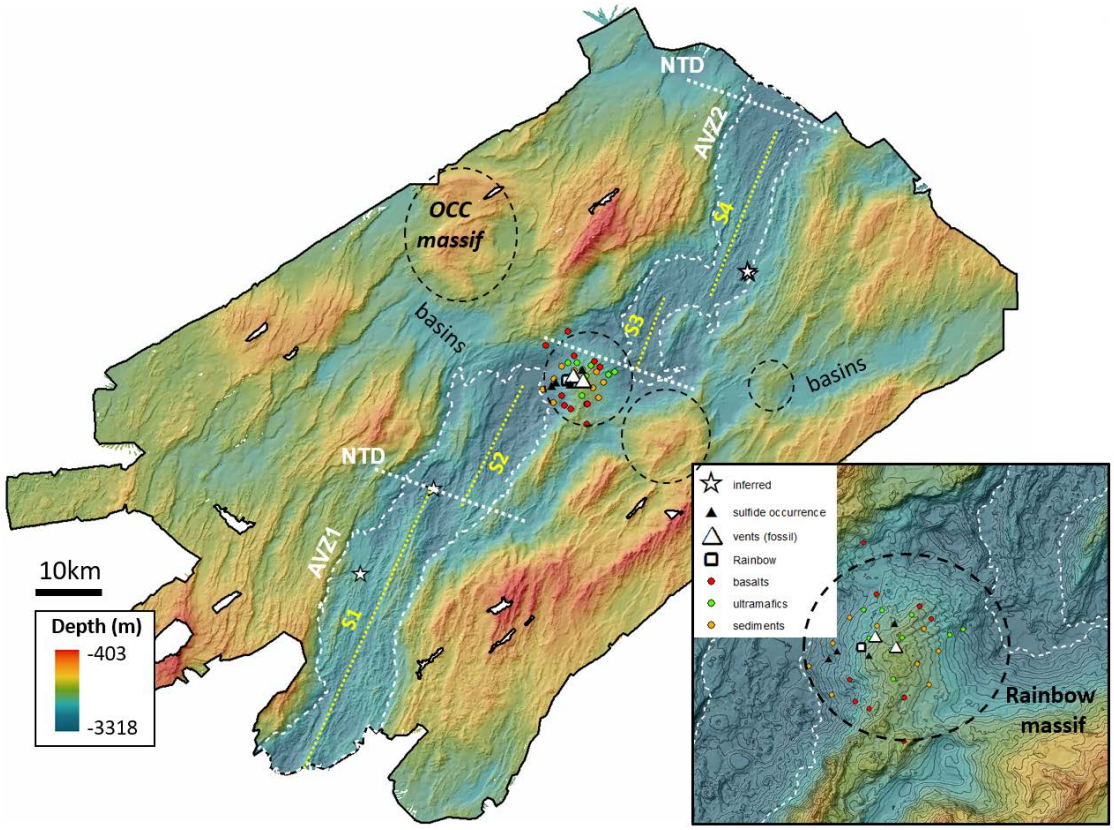

Figure 2. Bathymetric map of the surveyed Rainbow Area (data made available by Paulatto et al. 2015). The Rainbow massif and other massifs (dashed contours) represent remnants of oceanic core complexes (noted OCC). The ridge axis is marked by yellow dotted lines (segments S1, S2, S3 and S4) interpreted from the bathymetry (i.e. volcanic highs in the axial volcanic zones, or AVZ1 and AVZ2, delimited in dashed white contours). The three approximative ridge offsets (non-transform discontinuities, or NTDs) delimiting the ridge segments are indicated as dotted white

This activity has received funding from the European Institute of Innovation and Technology (EIT), a body of the European Union, under the Horizon 2020, the EU Framework Programme for Research and Innovation

lines. The rainbow hydrothermal field is marked with white square (active vent) and triangles (fossil vents). The location of other identified hydrothermal sites or plumes are marked with white stars (InterRidge Vents Database 3.2, http://vents-data.interridge.org/). Basins: flat terrain presumably highly sedimented.

This activity has received funding from the European Institute of Innovation and Technology (EIT), a body of the European Union, under the Horizon 2020, the EU Framework Programme for Research and Innovation

6. Available data

Data of the Rainbow Area were collected as part of the MARINER (Mid-Atlantic Ridge Integrated Experiments at Rainbow) marine geophysical survey of the Rainbow area (Dunn et al., 2013; Canales et al., 2013), and were made available online by Paulatto et al. (2015). Examples of data are the bathymetry (Fig.2), backscatter data (Fig.4), residual mantle bouguer anomaly and reduced-to-pole magnetic anomaly (Fig.3). This report makes essentially use of bathymetric mapping and interpretation of seafloor structures (e.g., fault signatures, volcanic highs and detachment surfaces), which represent important factor for mineralization processes. The swath bathymetry data were collected with a Kongsberg EM-122 multibeam system along closely spaced profiles which provided redundant coverage over most of the survey area (see Paulatto et al., 2015 for details). The high density of soundings allowed gridding at a relatively fine grid interval of 0.00025°x0.00025° (about 25 m grid spacing). The resulting grid covers a 70x110 km2 area of the seabed. To aid the interpretation of geomorphological features, a range of morphometric features have been calculated in GIS from the bathymetry, including slope gradient, terrain illumination and roughness. Slope gradient can be used to identify faults due to their steep slopes (≥ 25°) (see Fig.4). Areas where crustal accretion is significantly tectonized, long-lived slip detachment faults can form oceanic core complexes (OCCs) producing fault angles as low as 10°-20°. Hummocky structures can be recognized using roughness, which is defined as the maximum of the differences between a central grid node and the surrounding nodes in the bathymetric grid.

This activity has received funding from the European Institute of Innovation and Technology (EIT), a body of the European Union, under the Horizon 2020, the EU Framework Programme for Research and Innovation

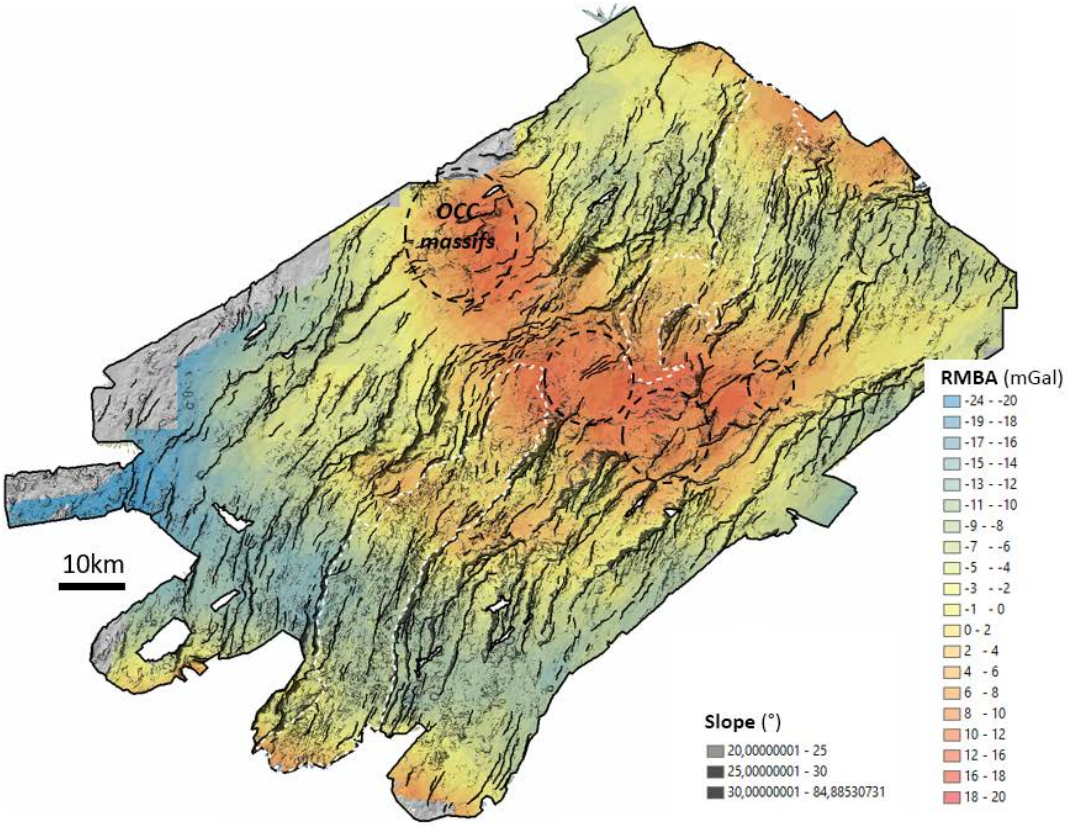

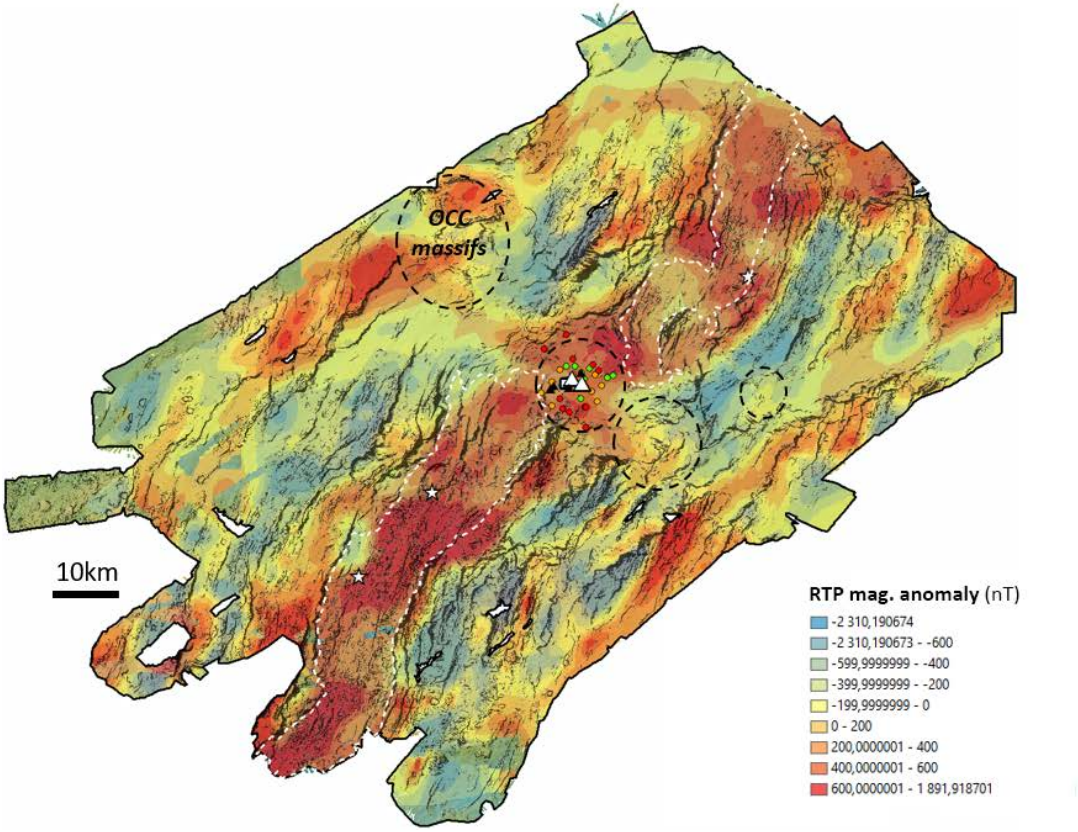

This activity has received funding from the European Institute of Innovation and Technology (EIT), a body of the European Union, under the Horizon 2020, the EU Framework Programme for Research and Innovation

Figure 3. Residual mantle bouguer anomaly (RMBA) used as proxy for crustal thickness and compositional variations (top) and reduced-to-pole magnetic anomaly (bottom).

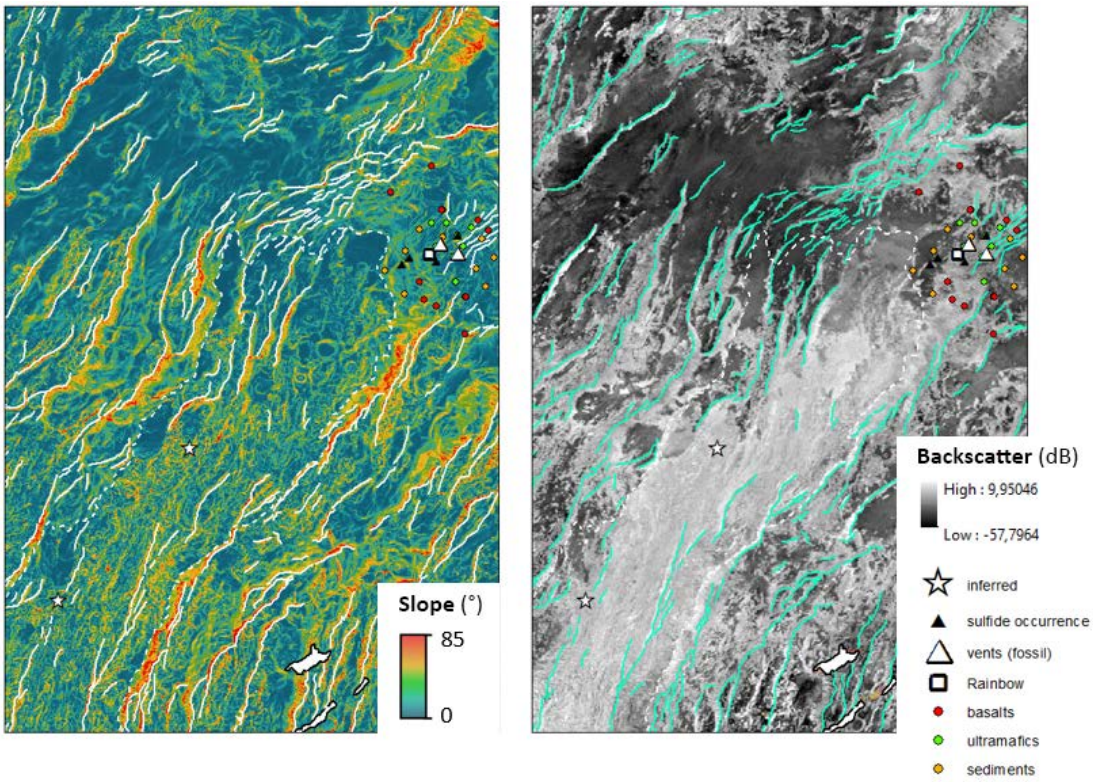

Figure 4. Fault crests interpreted from slope map (left) and backscatter data (right).

This activity has received funding from the European Institute of Innovation and Technology (EIT), a body of the European Union, under the Horizon 2020, the EU Framework Programme for Research and Innovation

7. Permissive tracts

Permissive tracts represent extended frontiers of terrains for which geologic environments permit a deposit type to form (Singer, 1993). Beyond those frontiers, the probability of occurrence for new findings is negligible for the deposit type considered. Inside the tracts, the deposit targets previously generated restrict mineral exploration into in-situ areas like the predefined deposit model. Hence, the tracts shall include the morpho-structural units and seafloor properties which comply with the model definition.

For consistency and simplification, the delineation of the tract boundaries is traced following the recognizable extents of volcanic terrain which represent the total area without the detachment and sedimented zones (Fig.5). As the ridge valley floor presents segmentation patterns and variable terrains, this delineation preserves the general elevated topography by taking away the flattened terrain not affected by disrupting structures, i.e., those usually considered as hosting sediment covers, and lacking fault signatures. Hence, predicted numbers of deposits are considered associated with ancient and volcanically active terrains.

The permissive tract area covers 7654 km2 (about the area of Puerto Rico) accounting for approximately 82% of the overall Rainbow Area seafloors.

This activity has received funding from the European Institute of Innovation and Technology (EIT), a body of the European Union, under the Horizon 2020, the EU Framework Programme for Research and Innovation

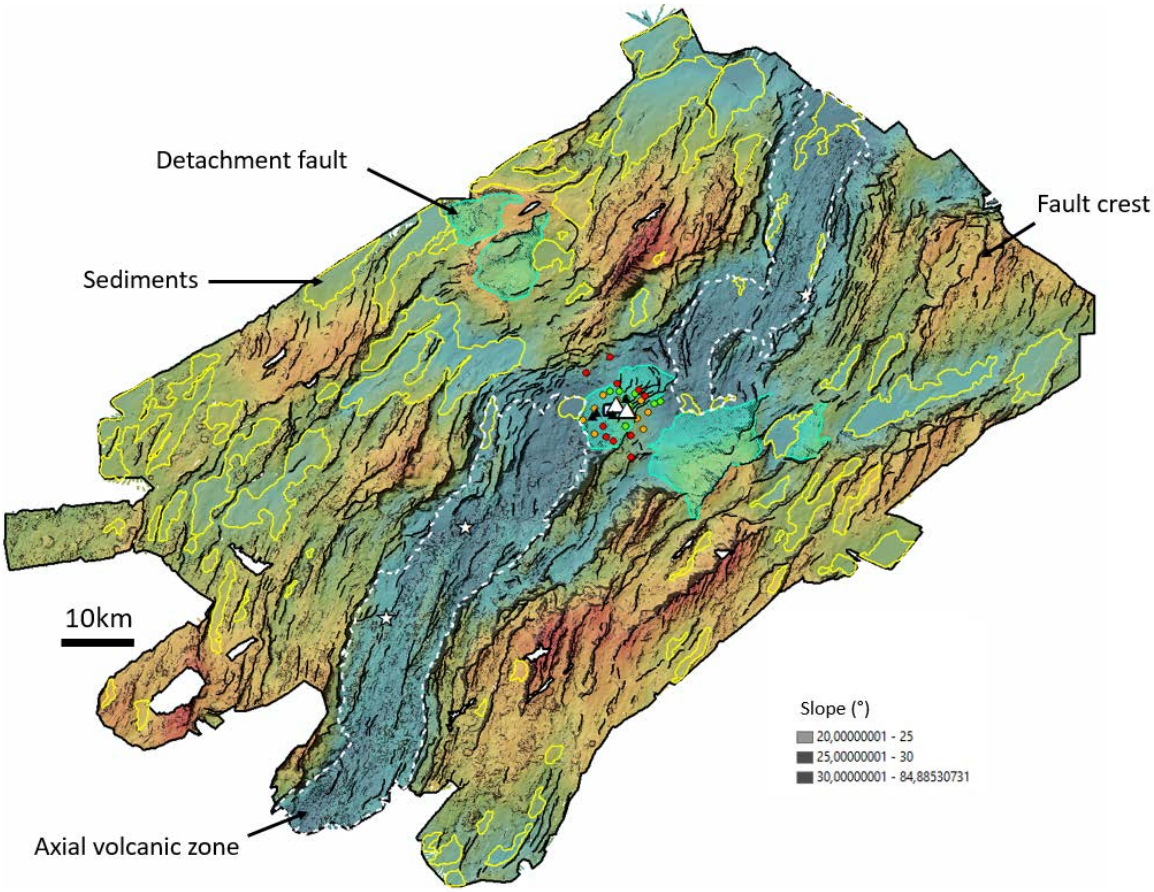

Figure 5. Seafloor classification based on bathymetry, topographic properties (slope, aspect and roughness) and results from simulated shading. Terrain not associated to sedimented zones and detachment fault surfaces correspond to basalt-related permissive tracts (7,654 km2).

This activity has received funding from the European Institute of Innovation and Technology (EIT), a body of the European Union, under the Horizon 2020, the EU Framework Programme for Research and Innovation

8. Deposit model

Available geoscience information about analogue deposits (e.g., ore distribution, abundance and quality) can be integrated into a system (deposit model) that serves as an estimation guide. The deposit model allows differentiating geologic settings among the deposit types studied and depict specific grade-tonnage-density distributions. In practice, a certain type of deposit is considered, and prospective areas are delineated according to the type(s) of deposit(s) permitted by the geology (Singer and Menzie, 2010). The SMS deposit model used in this report is presented in Table 1.

Table 1. Simplified descriptive model for Cu-Zn seafloor massive sulfide deposits at neo-volcanic terrains of sediment-starved MORs. A glossary of descriptive terminologies can be found in Singer and Menzie (2010).

Description: Cu-Zn sulfide deposits hosted in mafic rocks typically described as mid-ocean ridge basalts (MORBs) at active vent fields such as the TAG (26°30'N; Hannington et al., 1991; Rona et al., 1993; Humphris and Cann, 2000), Snakepit (23°37'N; Hannington et al., 1991; Fouquet et al., 1993; Krasnov et al., 1995) and Broken Spur (29°10'N; Murton et al., 1994; Duckworth, 1995) at the Mid-Atlantic Ridge.
Host rock: Pillow lavas.
Textures: Brecciated massive ore heavily textured by sulfide minerals, transiting at depth to a sulfide-silicate stockwork. The massive ore constitutes a mix of collapsed chimney fragments and finely interbedded sulfides, settling out from black smoker plumes (Hannington et al., 1998).
Age range: Few thousands to more than hundred thousand of years (Lalou et al., 1995; Cherkashov et al., 2016).
Depositional environment: Deep high-temperature venting sites, usually between 2,000 and 3,000 m (about the height of Mount St. Helens) depth below sea surface (Hannington et al., 2010) along the ridge crest or neo-volcanic terrains of axial valleys at oceanic spreading centers.
Tectonic setting: At divergent plate boundaries where rising and decompressing of solid mantle initiate melting and formation of new oceanic crust.

This activity has received funding from the European Institute of Innovation and Technology (EIT), a body of the European Union, under the Horizon 2020, the EU Framework Programme for Research and Innovation

Associated deposit type(s): Cu-Zn seafloor massive sulfide deposits with submarine-hydrothermal origin and generated through volcanic-*exhalative* processes.
Alteration: Alteration is typically zoned from the core stockwork zone to outward zones by (1) a silica-rich alteration zone replacing the host-rock with in-situ chalcopyrite-pyrite assemblages, (2) a chloritic alteration zone consisting of chlorite, opal, quartz ± sericite, (3) a sericitic alteration zone with sericite, ± chlorite, ± silica, and (4) a silicification zone often gradational with silica-albite metasomatism (Bonnet and Corriveau, 2007).
Ore minerals: Orebodies with, in decreasing order, different proportions of e.g., pyrite (FeS2) + chalcopyrite (CuFeS2) + sphalerite (ZnS) ± galena (PbS). Quartz + chlorite ± anhydrite ± barite represent among the principal gangue minerals. Clay minerals and calcite appear lately in the mineralization process as veinlets (Hannington et al., 1998).
Ore control: Thermally driven hydrothermal circulation within mafic oceanic crust; sulfide precipitation is controlled by prominent regional faults and local fracturing or cracks conducting upward focusing of hydrothermal fluid flow, venting and mineral accumulation at the seafloor (Franklin et al., 2005; Galley et al., 2007).
Weathering and sediment: Fe-rich oxides equivalent to ochreous and gossan materials capping the sulfide mound. Land-based evidence, such as sulfide deposits of the Troodos ophiolite, can present yellowish ochre (Fe-rich, Mn-poor sediment) attributed to sulfide weathering and oxidation (Robertson, 1976) and dark-brown umber (Fe- and Mn-rich sediment) generated from distal plume fall-out (Boyle, 1990).
Geochemical signatures: Sulfide mound with e.g., high Cu/(Cu+Zn) ratio in the vicinity of main high-temperature hydrothermal conduits, high Zn/(Cu+Zn) ratio among secondary fluid conduits (usually peripheral mound system), and a cap of Fe-rich (± Mn) oxide materials (Hannington et al., 1998).
Hydrographic signature: Seawater with e.g., varying temperature, salinity (NaCl), conductivity, turbidity and fluid compositions including trace elements of e.g., Cu, Zn, Pb, Co, Ni, Sr, and Se,

This activity has received funding from the European Institute of Innovation and Technology (EIT), a body of the European Union, under the Horizon 2020, the EU Framework Programme for Research and Innovation

and other volatiles such as methane (CH4), hydrogen (H2), carbon dioxide (CO2), hydrogen sulfide (H2S) and ammonium (NH4) (German and Von Damm, 2004).
Geophysical signature: Surveys using electromagnetic or self-potential, for example, can be used to map sulfide-rich and conductive rocks in the subsurface (e.g., Tivey and Johnson, 2002; Kowalczyk and Jackson, 2007; Kinsey et al., 2008; Kawada and Kasaya, 2017).

This activity has received funding from the European Institute of Innovation and Technology (EIT), a body of the European Union, under the Horizon 2020, the EU Framework Programme for Research and Innovation

9. Grade-tonnage models used in the assessment

Grade and tonnages models rely on lognormally distributed deposit size and commodity grades, where the logarithms of tonnage and grade of deposits are plotted versus the calculated proportion of the deposits. Grade-tonnage data distribution commonly show a positive skewness, and the mean and standard deviation of those data allow to fit a curve. To develop the distribution models, a compilation of quantitative historic information about the deposit type being studied is required. Ideally, such information is retrieved from well-explored deposits located in settings of geologic interest. The data in question include average grades of each metal of economic interest and the associated tonnage based on the total production, reserves and resource at the lowest possible cutoff grade (Singer and Menzie, 2010). Because available information is fragmented, the grades and tonnages used in this report are assumed to be statistically independent. The simulated tonnage has been truncated at maximum tonnage in the input data. Table 2 and Table 3 below give an overview of grades and tonnages found relevant to build the grade and tonnage models for the SMS case. These are from slow spreading settings and of Cyprus-type VMS deposits.

Table 2. Bulk chemical composition of selected Cyprus-type VMS deposits. Data given for Norway: McQueen (1990); Mosier et al. (2009); Albania: Hoxha et al. (2005); Mosier et al. (2009); Turkey: Çakir (1995); Yigit (2009); Yildirim et al. (2016); Oman: Savannah Resources Plc. (2014); Mosier et al. (2009); others: Mosier et al. (2009). Empty cells are undetermined values.

Country	Deposit	Cu (wt.%)	Zn (wt.%)	Au (ppm)	Ag (ppm)
Albania	Rubiku	2.01	0.7	0.5	
	Palai-Karme	2.48	0.9	0.4	
	Porave	2.15	1.4		
	Derven	0.98	0.24		
	Rehova	1.86	0.5	0.6	20
	Kachinar	3.85	1.55	0.5	12
	W Kachinar	1.45	0.8	0.5	12
Turkey	Ortaklar	2.32	0.32	0.735	5.365
	Toykondu	4		1.55	
	Anayatak (Ergani)	1.39			
	Mihrapdag (Ergani)	2.5		1.2	
	Siirt Madenkoy	1.55			
	Kure (Asikoy)	2.17		2.2	11
	Kure (Bakibaba)	2.2		1	

This activity has received funding from the European Institute of Innovation and Technology (EIT), a body of the European Union, under the Horizon 2020, the EU Framework Programme for Research and Innovation

Colombia	Sababablanca	5			
Canada	Chu Chua	2	0.4	0.44	8.66
	Sunro	1.23		0.144	1.45
	Huntingdon	0.9		0.1	0.6
Cuba	Cacarajicara	1.2			
	Jucaro	1.38			
Cyprus	Limni	1.4			
	Kokkinoyia	1.5	0.2		
	Ambelikou	1			
	Apliki	1.8			
	Kapedhes	0.5			
	Kokkinopezoula	0.5			
	Kynousa	2.04	1.7		
	Mavri Sykia-Landaria	2			
	Mousoulos-Kalavasos	1	0.5	1.7	6.1
	Peravasa	0.76			
	Petra	2			
	Platies	2			
	Sha	0.6			
	Agrokipia	1.7	1.09		
	Troulli	1			
	Skouriotissa	2.35	0.5		69
	Mathiati North	0.24	0.1		
	Mavrovouni	4	0.5	0.3	39
Guatemala	Oxec	3			
Norway	Lokken	2.1	1.9	0.3	19
	Dragset	2	2.5		20
Oman	Bayda	2			
	Lasail	2			
	Aarja	2			
	Carawison	2.8			
	Hatta (main)	3.41		0.3	
	Shinas	2			
Philippines	Carmel	1.48			
	Bongbongan	1.18			

This activity has received funding from the European Institute of Innovation and Technology (EIT), a body of the European Union, under the Horizon 2020, the EU Framework Programme for Research and Innovation

	Lorraine	4.5			
Russia	Osennee	4.69	0.24	0.3	20.8
	Letnee	3.3	1.55	0.6	13.7
	Bama	0.55			
	Fornas	1.33			
	Arinteiro	0.9			
Sweden	Viscaria	1.1			
United States	Threeman-Standard Copper	1.08		0.72	10.5
	Rua Cove	1.1			
	Western World	2.81	0.95	0.69	13.7

Table 3. Size of ophiolitic VMS deposits formed within a slow-spreading setting. Data given for Troodos: Mosier et al. (1986); Hannington et al. (1998); Adamides (2010); Mirdita: Hoxha et al. (2005).

Ophiolite	Deposit	Tonnage (Mt)
Troodos	Agrokipia A	0.765
	Agrokipia B	4.5
	Alestos	0.1
	Ambelikou	0.016
	Apliki	1.65
	East lefka	1.2
	Kalavassos	6
	Kambia	1.5
	Kapedhes	0.05
	Klirou East	0.42
	Klirou West	0.077
	Kokkinopezoula	3.5
	Kokkinoyia	0.5
	Kynousa	0.3
	Kynousa Uncle Charles	0.22
	Limni	16
	Mangaleni	0.1
	Mathiatis	2.8
	Mavri Sykia	0.376

This activity has received funding from the European Institute of Innovation and Technology (EIT), a body of the European Union, under the Horizon 2020, the EU Framework Programme for Research and Innovation

	Mavrovouni	15
	Memi	1.5
	Mousoulos	1.66
	Peravasa	0.09
	Peristerka	0.33
	Petra	0.526
	Phoenix	15
	Phoukasa	6
	Pitharokhoma	1.4
	Platies	0.045
	Sha	0.35
	Skouriotissa	5.44
	Troulli	0.27
Mirdita (west)	Rubiku	1.5
	Palai-Karme	2
	Porave	0.3
	Derven	1.6
	Rehova	5
	Kachinar	0.3
	W Kachinar	0.3

In the assessment runs, focus has been on Cu only. The grade and tonnage data given in the tables above have been plugged into the MAP-Wizard which produces possible grade and tonnage combinations of deposits that may be found inside the permissive tract. The resulting distributions are found in Fig.6 and Fig.7.

This activity has received funding from the European Institute of Innovation and Technology (EIT), a body of the European Union, under the Horizon 2020, the EU Framework Programme for Research and Innovation

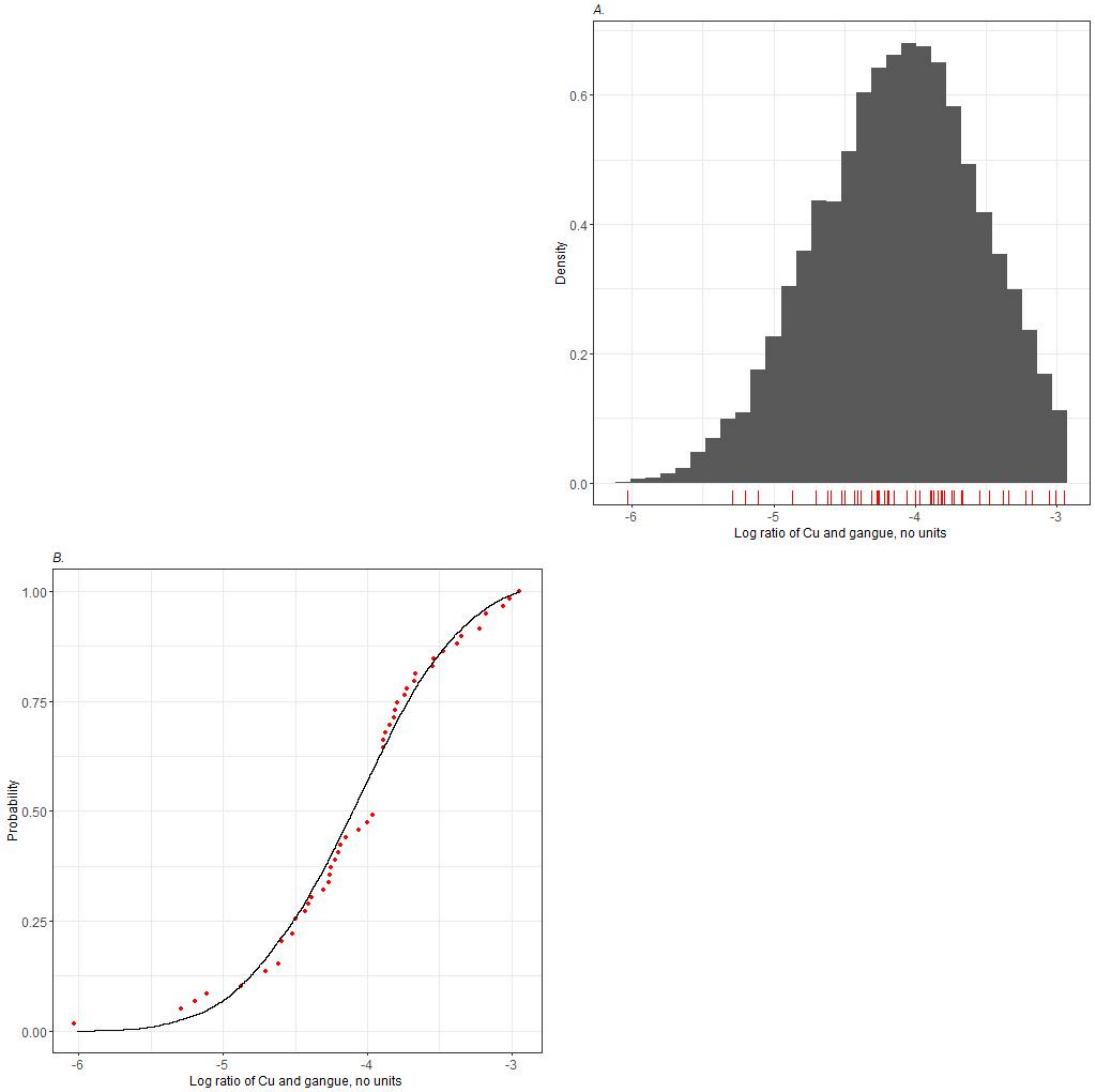

Figure 6. Probability density function (pdf, top) and cumulative distribution (bottom) of Cu.

This activity has received funding from the European Institute of Innovation and Technology (EIT), a body of the European Union, under the Horizon 2020, the EU Framework Programme for Research and Innovation

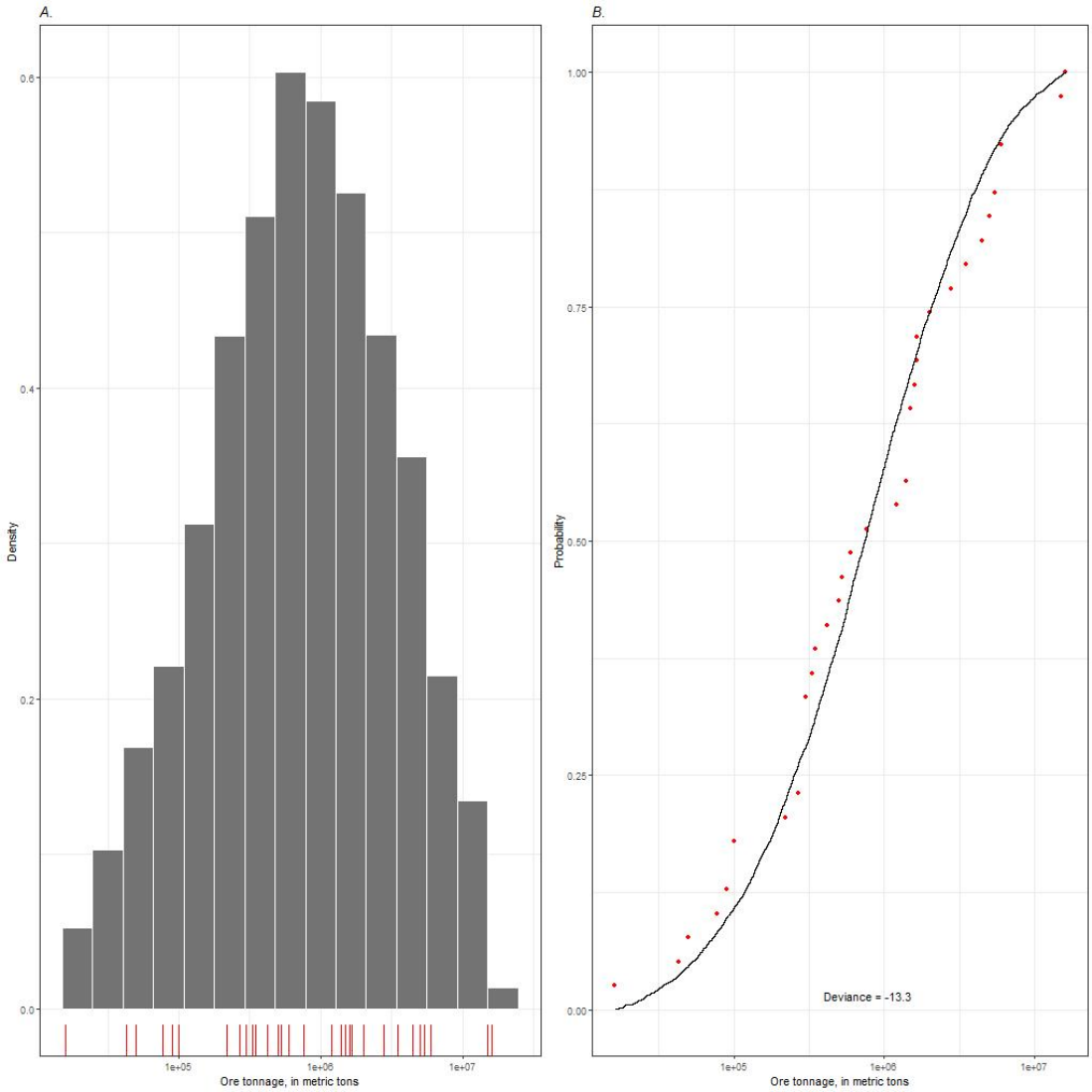

Figure 7. Probability density function (pdf, left) and cumulative distribution (right) of ore tonnage.

This activity has received funding from the European Institute of Innovation and Technology (EIT), a body of the European Union, under the Horizon 2020, the EU Framework Programme for Research and Innovation

10. Deposit density / number of deposits

In the Rainbow Area, undiscovered mineral deposits were estimated within volcanic terrains (7,654 km2), based on (1) the assumption that volcanic terrains are geologically favorable to the occurrence of SMS deposits (permissive tracts) and (2) a regressive law implemented in the MapWizard tool ("General model"; Fig.8), which was developed after the analysis of several deposit types from worldwide explored permissive tracts, evidencing a strong correlation between deposit size, permissive area, and deposit density over different prediction levels (10th, 50th and 90th percentiles) (Singer and Kouda, 2011):

$R_{50} = 4.2096 - 0.4987\ log_{10}area - 0.2252\ log_{10}size$	(1)
$L_{90},U_{10} = R_{50} \pm t\, S_{y\|s,a} \sqrt{\left(\frac{1 + 1/n + (3.175 - log_{10}\ area)^2(-0.3292 - log_{10}\ size)^2}{(n-1)S_s S_a}\right)}$	(2)

where R_{50} corresponds to the 50th percentile in the estimates of deposit density (deposit per 100,000 km2), L_{90} and U_{10} represent the 90th and 10th percentiles respectively for the density of deposits, t is the Student's t parameter, is the standard deviation of logarithmic values of deposit density given permissive area and deposit size, n is the number of permissive tracts studied worldwide, 3.175 is the mean logarithmic values of permissive tract area in square kilometers, -0.3292 is mean of logarithmic values of deposit tonnage in millions on metric tons in control tracts, 2.615 is the standard deviation of log-transformed deposit tonnages in permissive tracts, and 1.188 is standard deviation of logarithmic values of area of permissive tracts.

As the estimates from the equations (1) and (2) are initially re-scaled for 100,000 km2, densities are thus adjusted for the size of the tracts by multiplying them with the factor permissive area / 100,000 km2. Estimates on the number of deposits can then be calculated at the three different percent levels, using the estimated values as exponents to the power of 10:

$N = (permissive\ area/100{,}000) * 10^{\log_{10}(Density)}$	(3)

This activity has received funding from the European Institute of Innovation and Technology (EIT), a body of the European Union, under the Horizon 2020, the EU Framework Programme for Research and Innovation

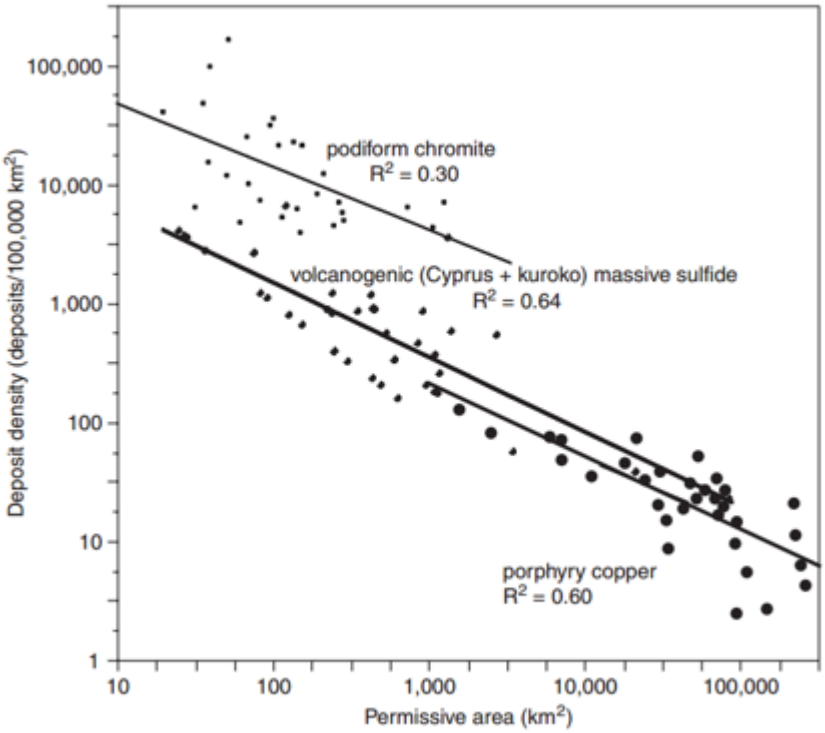

Figure 8. Density of deposits/100,000 km2 (about the area of Ohio) versus the permissive area (in km2): podiform chromite deposits, volcanogenic massive sulfide deposits (Cyprus and Kuroko types), and porphyry copper deposits with their respective regression lines. See Singer and Menzie, 2010 for details.

Given an expected median accumulation size of 0.765 Mt and a tract area of 7,654 km2, the P50 (median) number of undiscovered accumulations is 15. This means that we are 50% confident that there are 15 or more accumulations inside the tract. Values for N10 and N90 are given below in Fig.9.

This activity has received funding from the European Institute of Innovation and Technology (EIT), a body of the European Union, under the Horizon 2020, the EU Framework Programme for Research and Innovation

Number of undiscovered

deposits	Confidence
41	10%
15	50%
5	90%

Model: General
Median deposit tonnage (Mt): 0.765
Tract area (km2): 7654
Number of known deposits: 0

Figure 9. Number of deposits at different confidence levels. Although the Rainbow field, which belongs to the ultramafic setting, is a known accumulation / manifestation, the number of known deposits is equal to zero because it is the mafic setting that is assessed.

The number of deposits were also according to the 3-Part assessment procedure assessed using expert opinions. Experts were asked to assess the number of undiscovered deposits they were 10% (N10), 50% (N50) and 90% (N90) confident that there are present inside the tract. The results are presented as XY-plots in Fig.10 And Fig.11:

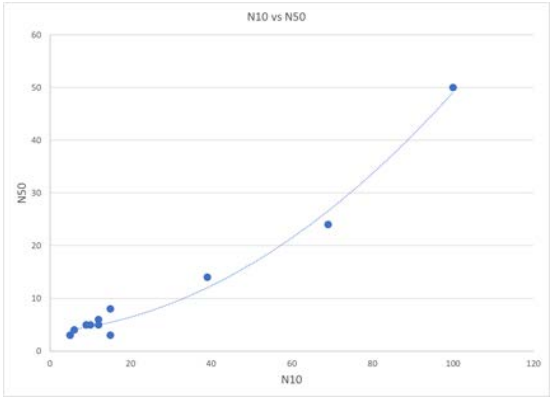

Figure 10. Number of deposits at N10 and N50 confidence levels.

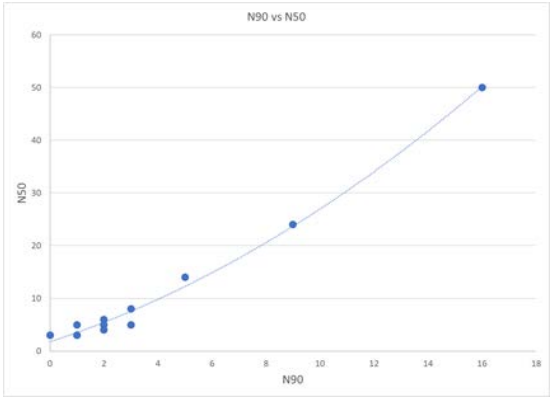

Figure 11. Number of deposits at N90 and N50 confidence levels.

This activity has received funding from the European Institute of Innovation and Technology (EIT), a body of the European Union, under the Horizon 2020, the EU Framework Programme for Research and Innovation

Table 4 summarizes the feedback from the experts that are presented graphically in Fig.10 and Fig.11. The variation in expert predictions is large with a long tail towards higher values, i.e. the majority of the assessors predict a relatively small number of deposits.

Table 4. Expert opinion summary statistics. The table illustrates how different the different experts have assessed the number of deposits which emphasize the great uncertainty.

	N90	N50	N10
Min	0.0	3.0	5.0
Max	16.0	50.0	100.0
Mean	3.8	10.8	24.8
Median	2.0	5.0	12.0
Standard deviation	4.54	13.76	30.05

Given the expert opinions, the MAP-Wizard tool develops negative binomial distributions. The probability density function (pdf) and the cumulative distribution function (cdf) are given in Fig.12.

This activity has received funding from the European Institute of Innovation and Technology (EIT), a body of the European Union, under the Horizon 2020, the EU Framework Programme for Research and Innovation

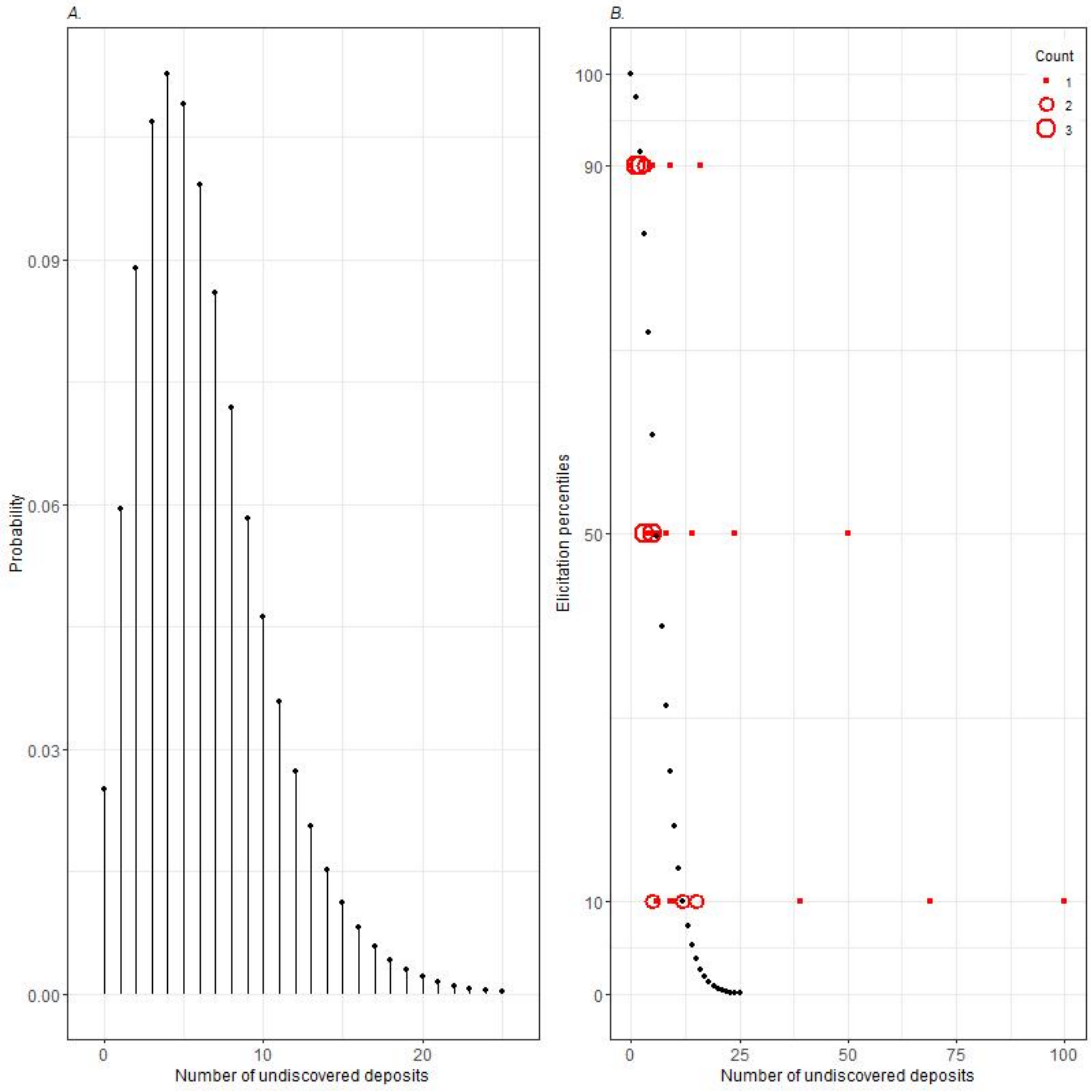

Figure 12. The probability density function (pdf, left) and the cumulative distribution function (cdf, right) describing the combined expectation from the experts and the associated uncertainty.

The results presented in Fig.12 (left) show that there is approximately a 2% chance that there are no deposits within the permissive tract. Further, this plot shows that the most likely number of deposits are between 4 to 6. Fig.12 (right) show that there is a 10% probability that that the number of deposits is higher than 15. These values are significantly lower than the values from the general model.

This activity has received funding from the European Institute of Innovation and Technology (EIT), a body of the European Union, under the Horizon 2020, the EU Framework Programme for Research and Innovation

11. Assessment results

Fig.13 shows the probability density function and the cumulative distribution function for the ore (not "ore" in the economic sense because it is not possible to assess how mineable a deposit in this region would be) and Cu metal tonnages.

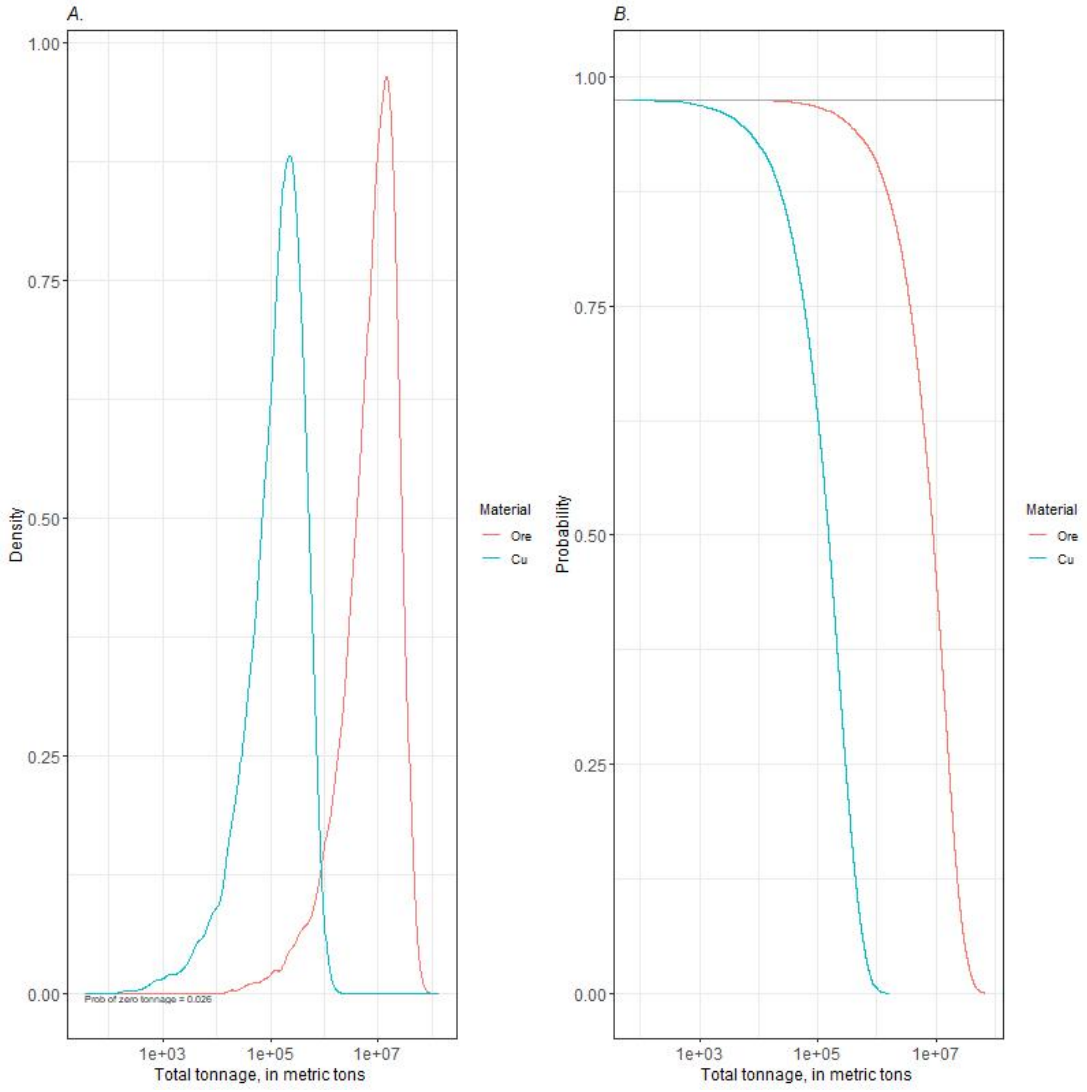

Figure 13. The probability density function (pdf, left) and the cumulative distribution function (cdf, right) describing the combined expectation from the experts and the associated uncertainty

This activity has received funding from the European Institute of Innovation and Technology (EIT), a body of the European Union, under the Horizon 2020, the EU Framework Programme for Research and Innovation

The results presented in Fig.13 is summarised in Table 5. The predicted expected value is 11.4 Mt of "ore" associated to the mafic setting yet to be found inside the Rainbow area. These deposits would contain 0.21 Mt of Cu. There is a probability of 95% that the "ore" tonnage is 0.31 Mt (5% chance that the ore tonnage is at least 0.31 Mt) or more. The median tonnage (Q_0.5 in the table) is 8.89 Mt.

The probability that the actual "ore" tonnage is above the mean is 40% and the probability that the "ore" tonnage is equal to zero is 2.6%. This stems from the probability of having no deposits (See Fig.12).

Table 5. Summary statistics showing the tonnage percentiles for the estimated resource potential

	Ore Mt	Cu Mt
Q_0.05	0.31	0.0046
Q_0.1	1.08	0.017
Q_0.25	3.63	0.06
Q_0.5	8.89	0.15
Q_0.75	16.50	0.29
Q_0.9	24.90	0.48
Q_0.95	30.90	0.61
Mean	11.40	0.21
P(0)	0.026	0.026
P(>Mean)	0.404	0.384

The tonnage marginals are included in Fig.14. The marginals show the discrete distribution of simulated deposits and the XY-plots show the correlation between the ore- and metal tonnages. The link between them is nothing else but the simulated grade.

This activity has received funding from the European Institute of Innovation and Technology (EIT), a body of the European Union, under the Horizon 2020, the EU Framework Programme for Research and Innovation

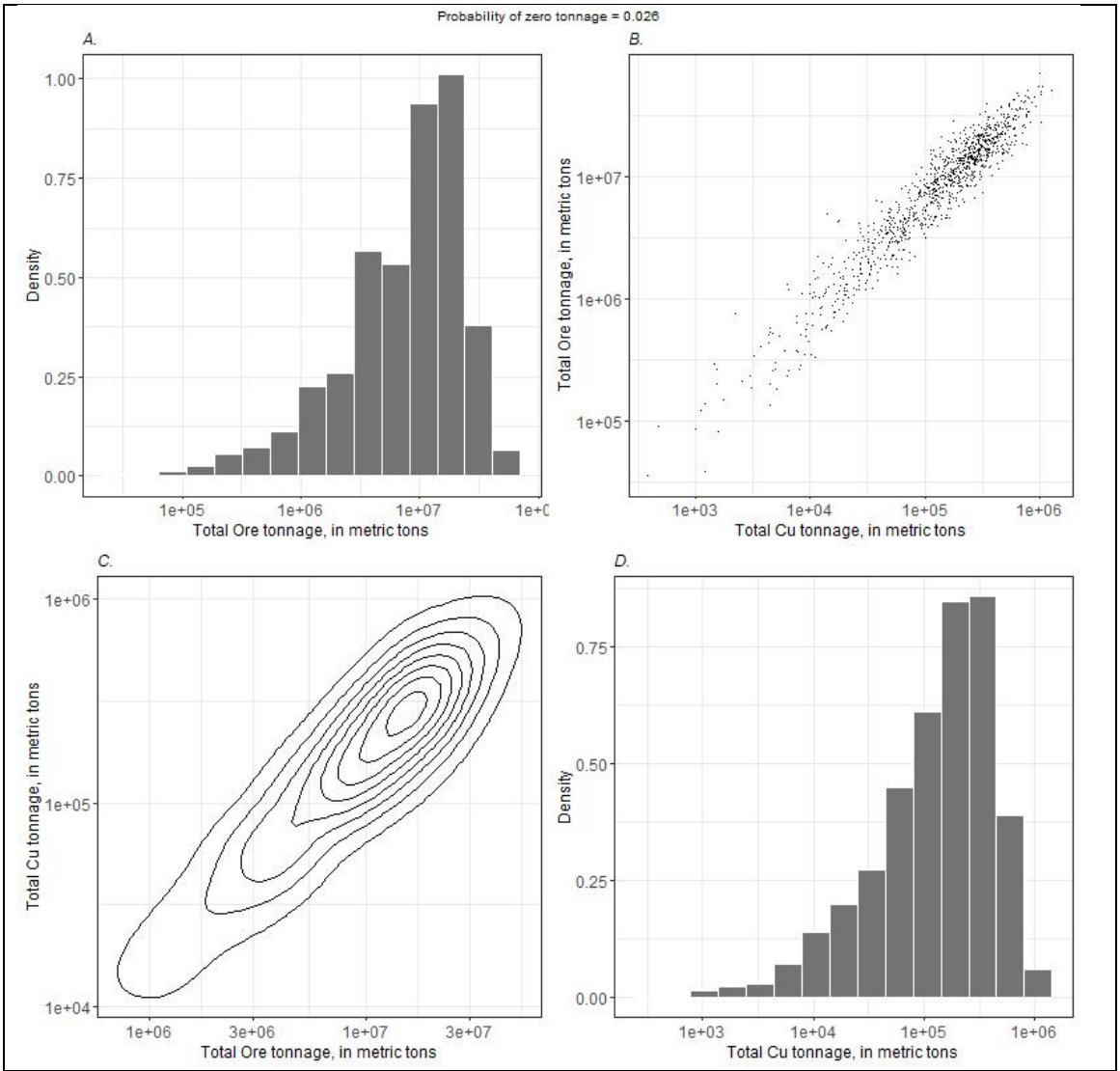

Figure 14. The figure shows the histograms and the XY-plots of the total ore and metal (Cu) tonnages. As indicated, there is a 2.6% probability to have zero tonnage. This originates from the number of deposit distribution in Fig.12.

This activity has received funding from the European Institute of Innovation and Technology (EIT), a body of the European Union, under the Horizon 2020, the EU Framework Programme for Research and Innovation

12. Discussion and future work

The play analysis takes a mineral system approach and aims at estimating factors that quantify how effective the required ore forming processes like energy, source, leaching, fluid migration and trapping are in a specific area (a permissive tract). The basis for this evaluation is the descriptive model (see chapter 8 for the descriptive model used in this project) that also forms the basis for the 3 Part assessment procedure which is the basis for the development of the MAP-Wizard tool. The MAP-Wizard includes so-called Mineral Prospectivity Mapping (MPM) techniques. These techniques take advantage of methodologies capable of finding patterns in multi-layered data. MPM techniques used onshore use e.g., geophysical, geochemical, and geological data. These data are mostly not available with the required resolution from the deep ocean floor and other data sources must be utilized. These are primarily bathymetry and relevant derivatives, but geophysical and backscatter data are of uttermost importance and are getting increasingly available.

The permissive tract is defined as an area where there is a negligible probability of finding a deposit outside the area. The available models for the number of deposits are based on this definition. If MPM techniques are included as an integrated part of the 3-part assessment and the definition of the tracts are based on other criteria than the models, then care must be taken. Applying MPM on tracts might render the general density models useless and one would have to rely fully on expert opinions.

We see from the assessment workshop executed on the SMS case that the prediction of the number of deposits (manifestations) vary greatly. The reason for this is primarily the varying level of knowledge about these systems and the assessment process. A two half days workshop is not enough to bring everyone on the same level and in a real implementation everyone would be given the opportunity to defend and to change the prediction of the number of undiscovered deposits.

A resource is some accumulation in the ground that potentially can be mined. A reserve is an accumulation that can be mined today, with today's technology, laws, and regulation and commodity prizes. The grade tonnage models are based on deposits that have been mined or fully explored. These models therefore already imply a mining method and a cost structure and would from this reason be truncated. The cost structures change with time and technological advances and future research and development should therefore aim at developing grade and tonnage models that truly quantify the resource potential and not some semi-reserve potential.

This activity has received funding from the European Institute of Innovation and Technology (EIT), a body of the European Union, under the Horizon 2020, the EU Framework Programme for Research and Innovation

13. Conclusions

Between 4 and 6 hydrothermal manifestations in the area comply with the defined grade and tonnage model. One could expect that these 4 to 6 deposits on average contain 13.6 Mt @ a median Cu-grade of 2wt%. The permissive area makes up 82% of the total Rainbow area.

The analysis shows that there is an average potential of yet to find resources (not classified according to USGS (2009) or similar classification schemes) of 11.4 Mt of ore (not in the economic sense of the term) and 0.2 Mt of Cu associated to a mafic (basalt-hosted) setting. However, the associated uncertainty is significant and future developments should for example aim at developing more reliable grade tonnage models for these kinds of deposits.

The MAP-Wizard facilitates the assessment process significantly and assist in increasing the transparency of the entire process. However, it is the input that makes the potential assessment reliable or not.

This activity has received funding from the European Institute of Innovation and Technology (EIT), a body of the European Union, under the Horizon 2020, the EU Framework Programme for Research and Innovation

14. References

Adamides, N., 2010. Mafic-dominated volcanogenic sulphide deposits in the Troodos ophiolite, Cyprus Part 2 - A review of genetic models and guides for exploration. Applied Earth Science: Transactions of the Institutions of Mining and Metallurgy, Section B 119: 193-204.

Adamides, N.G., 2010a. Mafic-dominated volcanogenic sulphide deposits in the Troodos ophiolite, Cyprus Part 1–The deposits of the Solea graben. Applied Earth Science: Transactions of the Institutions of Mining and Metallurgy: Section B 119, 65-77.

Adamides, N.G., 2010b. Mafic-dominated volcanogenic sulphide deposits in the Troodos ophiolite, Cyprus Part 2 - A review of genetic models and guides for exploration. Applied Earth Science: Transactions of the Institutions of Mining and Metallurgy: Section B 119, 193-204.

Allen, D. E., and W. E. Seyfried Jr., 2004. Serpentinization and heat generation: Constraints from Lost City and Rainbow hydrothermal systems, Geochim. Cosmochim. Acta., 68(6), 1347–1354, doi:10.1016/j.gca.2003.09.003.

Andreani, M., J. Escart[1]ın, A. Delacour, B. Ildefonse, M. Godard, J. Dyment, and Y. Fouquet (2014), Tectonic structure, lithology, and hydrothermal signature of the Rainbow massif (Mid-Atlantic Ridge 36°14'N), Geochem. Geophys. Geosyst., 15, 3543–3571, doi:10.1002/2014GC005269.

Attanasi, E. D., & Freeman, P. A., 2009. Economics of undiscovered oil and gas in the North Slope of Alaska; Economic update and synthesis: U.S. Geological Survey Open-File Report 2009-1112. Available online at: https://pubs.usgs.gov/of/2009/1112/pdf/ofr2009-1112.pdf

Barrie, C.T., and Hannington, M.D., 1999. Volcanic-associated massive sulfide deposits: Processes and examples in modern and ancient settings. Reviews in Economic Geology Volume 8, Society of Economic Geologists, Denver, 408 p.

Bonnet, A.-L., and Corriveau, L., 2007. Alteration vectors to metamorphosed hydrothermal systems in gneissic terranes, in Goodfellow, W.D., ed., Mineral deposits of Canada - A synthesis of major deposit-types, district metallogeny, the evolution of geological provinces, and exploration methods. Geological Association of Canada, Mineral Deposits Division, Special Publication No. 5, 1035-1049.

This activity has received funding from the European Institute of Innovation and Technology (EIT), a body of the European Union, under the Horizon 2020, the EU Framework Programme for Research and Innovation

Çakir, Ü., 1995. Geological characteristics of the Aşiköy-Toykondu (Küre-Kastamonu) massive sulfide deposits. Mineral. Res. Expl. Bull., 117, Ankara, pp. 29-40.

Canales, J. P., et al., 2013. MARINER: Seismic Investigation of the Rainbow Hydrothermal Field and its Tectono/Magmatic Setting, MidAtlantic Ridge 36814'N—A Report from RV M.G. Langseth Cruise MGL1305,InterRidge News, 22, 46–52.

Cann, J. R., and Strens, M.R., 1982. Black smokers fuelled by freezing magma,Nature, 298, 147–149, doi:10.1038/298147a0.

Cann, J., Gillis, K., 2004. Hydrothermal insights from the Troodos ophiolite, Cyprus. Hydrogeol. Ocean. Lithosphere, 1, 272.

Cann, J.R., Smith, D.K., Escartin, J., and Schouten, H., 2015. Tectonic evolution of 200 km of Mid-Atlantic Ridge over 10 million years: Interplay of volcanism and faulting. Geoch. Geoph. Geosyst., 16, 2303-2321.

Cherkashov, G., Kuznetsov, V., Kuksa, K., Tabuns, E., Maksimov, F., Bel'tenev, V., 2016. Sulfide geochronology along the Northern Equatorial Mid-Atlantic Ridge. Ore Geology Review, 87, 147-154.

Craig, J.R., and Vaughan, D.J., 1981. Ore Microscopy and Ore Petrography. John Wiley & Sons, New York, 406p.

Detrick, R. S., H. D. Needham, and V. Renard, 1995. Gravity anomalies and crustal thickness variations along the Mid-Atlantic Ridge between 338N and 408N,J. Geophys. Res., 100, 3767–3787, doi:10.1029/94JB02649.

Dilek, Y., and Robinson, P.T., eds., 2003. Ophiolites in Earth history. Geological Society of London Special Publication 218, 717p.

Dilek, Y., Moores, E.M., Elthon, D., and Nicolas, A., eds., 2000. Ophiolites and Oceanic Crust: New Insights from Field Studies and the Ocean Drilling Program: Geological Society of America Special Paper 349, 552p.

This activity has received funding from the European Institute of Innovation and Technology (EIT), a body of the European Union, under the Horizon 2020, the EU Framework Programme for Research and Innovation

Duckworth, R.C., Knott, R., Fallick, A.E., Rickard, D., Murton, B.J., Van Dover, C.L., 1995. Mineralogy and sulphur isotope geochemistry of the Broken Spur sulphides, 29°N, Mid-Atlantic Ridge. In: Parson LM, Walker CL, Dixon DR (eds) Hydrothermal vents and processes. Geological Society, London, 175-189 (Spec Pub geol Soc Lond No. 87).

Dunn, R. A., J. P. Canales, R. A. Sohn, M. Paulatto, R. Arai, and F. Szitkar, 2013. The MARINER Integrated Seismic and Geophysical Mapping Experiment, Abstract T21F-07 presented at 2013 Fall Meeting, AGU, San Francisco, Calif.

Dutton, S. P., Kim, E. M., Broadhead, R. F., Raatz, W., Breton, C., Ruppel, S. C., Kerans, C., & Holtz, M. H., 2003. Play analysis and digital portfolio of major oil reservoirs in the Permian Basin: Application and transfer of advanced geological and engineering technologies for incremental production opportunities. The University of Texas at Austin, Bureau of Economic Geology, and New Mexico Bureau of Geology and Mineral Resources, New Mexico Institute of Mining and Technology, annual report prepared for U.S. Department of Energy. Available online at: https://www.osti.gov/servlets/purl/825581

Escartin, J., Smith, D.K., Cann, J., Schouten, H., Langmuir, C.H., and Escrig, S., 2008. Central role of detachment faults in accretion of slow-spreading oceanic lithosphere. Nature, 455, 790-794.

Ellefmo, S. L., Søreide, F., Cherkashov, G., Juliani, C., Panthi, K. K., Petukhov, S., et al. (2019). *Quantifying the Unknown - Marine Mineral Resource Potential on the Norwegian Extended Continental Shelf*. Cappelen Damm Akademiske. https://doi.org/10.23865/noasp.81

Fialko, Y.A., and Rubin, A.M., 1998. Thermodynamics of lateral dike propagation: Implications for crustal accretion at slow spreading mid-ocean ridges. J. Geophys. Res. 103, 2501-2514.

Fouquet, Y., 1997. Where are the large hydrothermal sulphide deposits in the oceans? Royal Society of London Philosophical Transactions, ser. A, 355, 427-441.

Fouquet, Y., Cambon, P., Etoubleau, J., Charlou, J.L., Ondreas, H., Barriga, F.J.A.S., Cherkashov, G., Semkova, T., Poroshina, I., Bohn, M., Donval, J.P., Henry, K., Murphy, P., Rouxel, O., 2010. Geodiversity of hydrothermal processes along the Mid-Atlantic Ridge and ultramafic-hosted mineralization: A new type of oceanic Cu-Zn-Co-Au volcanogenic massive sulfide deposit. Article in Geophysical Monograph Series, 188, 321-367.

This activity has received funding from the European Institute of Innovation and Technology (EIT), a body of the European Union, under the Horizon 2020, the EU Framework Programme for Research and Innovation

Fouquet, Y., Wafik, A., Cambon, P., Mevel, C., Meyer, G., Gente, P., 1993. Tectonic setting and mineralogical and geochemical zonation in the Snake Pit sulfide deposit (Mid-Atlantic Ridge at 23°N). Econ. Geol., 88, 2018-2036.

Franklin, J.M., Gibson, H.L., Jonasson, I.R., and Galley, A.G., 2005. Volcanogenic massive sulfide deposits, in Hedenquist, J.W., Thompson, J.F.H., Goldfarb, R.J., and Richards, J.P., eds., Economic Geology 100th Anniversary Volume: The Economic Geology Publishing Company, 523-560.

Franklin, J.M., Sangster, D.M., and Lydon, J.W., 1981. Volcanic-associated massive sulfide deposits. Economic Geology 75th Anniversary Volume, 485-627.

Furnes, H., de Wit, M., and Dilek, Y., 2014. Four billion years of ophiolites reveal secular trends in oceanic crust formation. Geoscience Frontiers 5, 571-603.

Galley, A.G., Hannington, M.D., and Jonasson, I.R., 2007. Volcanogenic massive sulphide deposits. In: Goodfellow, W.D., ed., Mineral Deposits of Canada: A Synthesis of Major Deposit-Types, District Metallogeny, the Evolution of Geological Provinces, and Exploration methods. Geological Association of Canada, Mineral Deposits Division, Special Publication, 5, 141-161.

Galley, A.G., Koski, R.A., 1999. Setting and characteristics of ophiolite-hosted volcanogenic massive sulfide deposits. In: Barrie, C.T., and Hannington, M.D., Volcanic-associated massive sulfide deposits-Processes and examples in modern and ancient settings. Reviews in Economic Geology, 8, 221-246.

Gautier, D. L., Dolton, G. L., Takahashi, K. I., & Varnes, K. L., 1995. National assessment of US oil and gas resources. Overview of the 1995 national assessment. Results, methodology, and supporting data: US Geological Survey Digital Data Series 30 (available online).

German, C. R., A. M. Thurnherr, J. Knoery, J. L. Charlou, P. Jean-Baptiste, and H. N. Edmonds, 2010. Heat, volume and chemical fluxes from submarine venting: A synthesis of results from the Rainbow hydrothermal field, 368N MAR,Deep Sea Res., Part I, 57(4), 518–527, doi:10.1016/j.dsr.2009.12.011.

German, C.R., and Von Damm, K.L., 2004. Hydrothermal processes. In: Holland, H.D., Turekian, K.K. and Elderfield, H. (eds.) Treatise on geochemistry, Vol. 6. The oceans and marine geochemistry. Oxford, UK, Elsevier-Pergamon, 181-222.

This activity has received funding from the European Institute of Innovation and Technology (EIT), a body of the European Union, under the Horizon 2020, the EU Framework Programme for Research and Innovation

Gilgen, S.A., Diamond, L.W., Mercolli, I., Al-Tobi, K., Maidment, D.W., Close, R., Al-Towaya, A., 2014. Volcano-stratigraphic Controls on the Occurrence of Massive Sulfide Deposits in the Semail Ophiolite. Oman. Econ. Geol. 109, 1585-1610.

Hagemann, S. G., Lisitsin, V. A., & Huston, D. L., 2016. Mineral System. Analysis: Quo Vadis. Ore geology Reviews, 76, 504-22.

Hannington, M.D., 2014. Volcanogenic massive sulphide deposits. In: Holland, H.D., Turekian, K.K. (ed) Treatise on geochemistry 2nd edition. Elsevier Ltd, 319-350.

Hannington, M.D., Galley, A.G., Herzig, P.M., Petersen, S., 1998. Comparison of the TAG mound and stockwork complex with Cyprus-type massive sulphide deposits. In: Proceedings of the Ocean Drilling Program, Scientific Results, 158, 389-415.

Hannington, M.D., Herzig, P.M., Scott, S.D., Thompson, G., and Rona, P.A., 1991. Comparative mineralogy and geochemistry of gold-bearing sulfide deposits on the mid-ocean ridges. Mar. Geol. 101, 217-248.

Hannington, M.D., Jamieson, J., Monecke, T., Petersen, S., 2010. Modern sea-floor massive sulfides and base metal resources: toward an estimate of global sea-floor massive sulfide potential. Spec. Publ. Soc. Econ. Geol., 15, 317-338.

Hoxha, L., Scott, P.W., Eyre, J.M., 2005. The geological setting of volcanogenic sulphide orebodies in Albanian ophiolites. Applied Earth Science (Trans. Inst. Min. Metall.) 114: 33-52.

Hronsky, J. M. A., & Groves, D., 2008. Science of targeting: definition, strategies, targeting and performance measurement. Australian Journal of Earth Sciences, 55, 3-12.

Humphris, S.E., and Cann, J.R., 2000. Constraints on the energy and chemical balances of the modern TAG and ancient Cyprus seafloor sulfide deposits. J. Geophys. Res. 105, 28,477-28,488.

Kawada, Y., and Kasaya, T., 2017. Marine self-potential survey for exploring seafloor hydrothermal ore deposits. Scientific Reports, 7.

This activity has received funding from the European Institute of Innovation and Technology (EIT), a body of the European Union, under the Horizon 2020, the EU Framework Programme for Research and Innovation

Kinsey, J.C., Tivey, M.A., and Yoerger, D.R., 2008. Toward high-spatial resolution gravity surveying of the mid-ocean ridges with autonomous underwater vehicles: Oceans 2008 Marine Technology Society-Institute of Electrical and Electronics Engineers Conference, Quebec City, Canada, 15-18 September 2008, Proceedings, 10p.

Kowalczyk, P., and Jackson, E., 2007. The role of subsea geophysical exploration for SMS deposits: Oceans 2007 Marine Technology Society-Institute of Electrical and Electronics Engineers Conference, Vancouver, Canada, 29 September-4 October 2007, Proceedings, 4p.

Krasnov, S.G., Cherkashev, G.A., Stepanova, T.V., Batuyev, B.N., Krotov, A.G., Malin, B.V., Maslov, M.N., Markov, V.F., Poroshina, I.M., Samovarov, M.S., Ashadze, A.M., Lazareva, L.I., Ermolayev, I.K., 1995. Detailed geological studies of hydrothermal fields in the North Atlantic. Geol. Soc., Lond., Spec. Public. 87, 43-64.

Lalou, C., Reyss, J.L., Brichet, E., Rona, P.A., and Thompson, G., 1995. Hydrothermal activity on a 10^5-year scale at a slow-spreading ridge. TAG hydrothermal field, Mid-Atlantic Ridge 26°N. Journal of Geophysical Research 100, 17,855-17,862.

Large R.R., 1992. Australian volcanic-hosted massive sulfide deposits: features, styles, and genetic models. Economic Geology, 87(3), 471-510.

Macdonald, K.C., 1982. Mid-ocean ridges: Fine scale tectonic, volcanic and hydrothermal processes within the plate boundary zone. Ann. Rev. Earth Planet. Sci., 10, 155-90.

McCuaig, T. C., Hronsky, J. M. A., 2014. The mineral system concept: the key to exploration targeting. Society of Economic Geologists Special Publication, 18, 153-175.

McQueen, K.G., 1990. The Dragset copper-zinc deposit: a deformed, volcanogenic sulphide occurrence in the Løkken greenstones, Central Norway. Norsk Geologisk Tidsskrift 70: 1-19.
Miyashiro, A., 1973. The Troodos ophiolite complex was probably formed in an island arc. Earth Planet. Sci. Lett. 19, 218-224.

Mosier, D.L., Berger, V.I., Singer, D.A., 2009. Volcanogenic massive sulfide deposits of the world: Database and grade and tonnage models. Open-File Report 2009-1034, U.S. Department of the Interior/U.S. Geological Survey, 50p.

This activity has received funding from the European Institute of Innovation and Technology (EIT), a body of the European Union, under the Horizon 2020, the EU Framework Programme for Research and Innovation

Mosier, D.L., Singer, D.A., and Salem, B.B., 1986. Geologic and grade-tonnage information on volcanic-hosted copper-zinc-lead massive sulfide deposits. U.S. Geological Survey Open-File Report 83-89, 78 p.

Murton, B.J., Klinkhammer, G., Becker, K., Briais, A., Edge, D., Hayward, N., Millard, N., Mitchell, I., Rouse, I., Ridnicki, M., Sayanagi, K., Sloan, H., Parson, L., 1994. Direct measurements of the Distribution and Occurrence of Hydrothermal Activity Between 27 and 30 degrees north on the Mid-Atlantic Ridge. Earth Planet. Sci. Lett. 125, 119-128.

Nicolas, A., 1989. Structures of ophiolites and dynamics of ocean lithosphere, Kluver, Dordrecht, 367 pp.

Parson, L., E. Gracia, D. Coller, C. German, and D. Needham , 2000. Second-order segmentation; the relationship between volcanism and tectonism at the MAR, 38°N-35°40'N, Earth Planet. Sci. Lett., 178(3), 231–251, doi:10.1016/S0012-821X(00)00090-X

Paulatto, M., Canales, J.P., Dunn, R.A., Sohn, R.A., 2015. Heterogeneous and asymmetric crustal accretion: New constraints from multibeam bathymetry and potential field data from the Rainbow area of the Mid-Atlantic Ridge (36815'N). Geochem. Geophys. Geosyst., 16, 2994–3014.

Pearce, J.A., Lippard, S.J., and Roberts, S., 1984. Characteristics and tectonic significance of supra-subduction zone ophiolites. J. Geol. Soc. London, 16, 77-94.

Robertson, A.H.F., 1976. Origins of ochres and umbers: Evidence from Skouriotissa, Troodos massif, Cyprus. Institute of Mining and Metallurgy Transactions, Section B, 85, 245-251.

Rona, P.A., and Scott, S.D., 1993. Seafloor hydrothermal mineralization: New perspectives: Economic Geology and the Bulletin of the Society of Economic Geologists, 88, 1935-1976.

Rona, P.A., Klinkhammer, G., Nelsen, T.A., Trefry, J.H., and Elderfield, H., 1986. Black smokers, massive sulphides and vent biota at the Mid-Atlantic Ridge. Nature, 321.

Savannah Resources Plc, 2014. Savannah Expands into the Highly Prospective Oman Copper Belt. Available online at: https://www.rns-pdf.londonstockexchange.com/rns/5510E_-2014-4-10.pdf

This activity has received funding from the European Institute of Innovation and Technology (EIT), a body of the European Union, under the Horizon 2020, the EU Framework Programme for Research and Innovation

Shanks, W.C. Pat, III and Thurston, R., 2010. Volcanogenic massive sulfide occurrence model: Chapter C, Mineral deposit models for resource assessment. USGS Scientific Investigations Report: 2010-5070-C.

Singer, D. A., 1993. Basic concepts in three-part quantitative assessments of undiscovered mineral resources. Non-Renewable Resources, 2 (2), 69-81.

Singer, D.A., Kouda, R., 2011. Probabilistic Estimates of Number of Undiscovered Deposits and Their Total Tonnages in Permissive Tracts Using Deposit Densities. Nat. Resour. Res. 20, 89-93.

Singer, D.A., Menzie, W.D., 2010. Quantitative mineral resource assessments, an integrated approach. Oxford University Press.

Smith, D. K., Schouten, H., Dick, J.B., Cann, J.R., Salters, V., Marschall, H.R., Ji, F., Yoerger, D., Sanfilippo, A., Parnell-Turner, R., Palmiotto, C., Zheleznov, A., Bai, H., Junkin, W., Urann, B., Dick, S., Sulanowska, M., Lemmond, P., Curry, S., 2014. Development and evolution of detachment faulting along 50 km of the Mid-Atlantic Ridge near 16.5°N. Geochem. Geophys. Geosyst. 15, 4692-4711.

Smith, D.K., and Cann, J.R., 1990. Hundreds of small volcanoes on the median valley floor of the Mid-Atlantic Ridge at 24°30'N. Nature, 348, 152-155.

Smith, D.K., Escartín, J., Schouten, H., and Cann, J.R., 2008. Fault rotation and core complex formation: Significant processes in seafloor formation at slow-spreading mid-ocean ridges (Mid-Atlantic Ridge, 13–25°N). Geochemistry Geophysics Geosystems 9, Q03003.

Thibaud R., P. Gente, and M. Marcia, 1998. A systematic analysis of the Mid-Atlantic Ridge morphology and gravity between 158N and 40 °N: Constraints of the thermal structure,J. Geophys. Res., 103, 24,201–24,221, doi:10.1029/97JB02934.

Tivey, M.A., and Johnson, H.P., 2002. Crustal magnetization reveals subsurface structure of Juan de Fuca Ridge hydrothermal vent fields. Geology, 30, 979-982.

USGS (2009). A resource/reserve classification for minerals. In Mineral Commodity Summaries Retrieved 20.05.2019 from http://minerals.usgs.gov/minerals/pubs/mcs/2009/mcsapp2009.pdf

This activity has received funding from the European Institute of Innovation and Technology (EIT), a body of the European Union, under the Horizon 2020, the EU Framework Programme for Research and Innovation

Wakabayashi, J., Dilek, Y., 2003. What constitutes 'emplacement' of an ophiolite?: Mechanisms and relationship to subduction initiation and formation of metamorphic soles. Geological Society of London Special Publication 217, 427-447.

White, D.A., 1988. Oil and gas play maps in exploration and assessment: AAPG Bulletin, 72 (8), 944-949.

White, D.A., 1993. Geologic risking guide for prospects and plays. AAPG Bulletin, 77, 2048–2061.

Wilson, M., 1989. Igneous Petrogenesis. A global tectonic approach, 101-104.

Yigit, O., 2009. Mineral deposits of Turkey in relation to Tethyan Metallogeny: Implications for future mineral exploration. Economic Geology 104(1): 19-51.

Yildirim, N., Dönmez, C., Kang, J., Lee, I., Pirajno, F., Yildirim, E., Günay, K., Seo, J.H., Farquhar, J., Chang, S.W., 2016. A magnetite-rich Cyprus-type VMS deposit in Ortaklar: A unique VMS style in the Tethyan metallogenic belt, Gaziantep, Turkey. Ore Geology Reviews 79: 425-442.

This activity has received funding from the European Institute of Innovation and Technology (EIT), a body of the European Union, under the Horizon 2020, the EU Framework Programme for Research and Innovation